Dear editor and referee#1,

Thank you very much for your time and attentions on this work. The comments and suggestions are very useful to improve our manuscript. Following is a point-by-point response to referee #1's comments. Texts in black are the comments, those in blue are our responses. All the line numbers mentioned in responses are referred to the manuscript with changes marked.

We hope that you will find the changes satisfactory and we are looking forward to hearing from you soon.

---

(1) In model validation (section 3.1), the authors compare the simulated $J[NO_2]$ with the observations. In addition to $J[NO_2]$, $J[O_3{}^1D]$ is also important in affecting the ozone photochemical production. Comparison on $J[O_3{}^1D]$ will show more sufficient evidence to demonstrating the well model performance in simulating photolysis rates. If the authors have the observations of $J[O_3{}^1D]$, please add the comparison of $J[O_3{}^1D]$.

Reply: Thank you for this comment. $J[O_3{}^1D]$ is indeed important in ozone photochemistry. Comparison on $J[O_3{}^1D]$ is important and necessary in photolysis rates validation. However, we didn't have the data before. Fortunately, we now have gathered the observations of $J[O_3{}^1D]$ at Xianghe station, and added the comparison of $J[O_3{}^1D]$ in the revised manuscript. Like the comparison of $J[NO_2]$, both the time series of $J[O_3{}^1D]$ and the relevant model performance metrics showed a good agreement between the observations and simulations. The model validations on $J[NO_2]$ and $J[O_3{}^1D]$ suggested that the WRF-Chem model performed very well in simulating the photolysis rates. Details can be checked in the revised manuscript in section 3.1.2.

(2) The authors showed that $J[NO_2]$ was enhanced at altitude above 1.3 km which is due to the enhancement of the light caused by the light-scattering effect of aerosols.

Discussions on the compositions of the aerosols and their effects on $J[NO_2]$ over this place are necessary. Please add them in the manuscript.

Reply: Thank you for your comment. Based on the optical properties of aerosols, they can be classified into light-scattering aerosols and light-absorbing aerosols. Before talking about the comprehensive effects of aerosols on $J[NO_2]$, it's necessary to present the effects of light-scattering aerosols and light-absorbing aerosols on $J[NO_2]$, respectively.

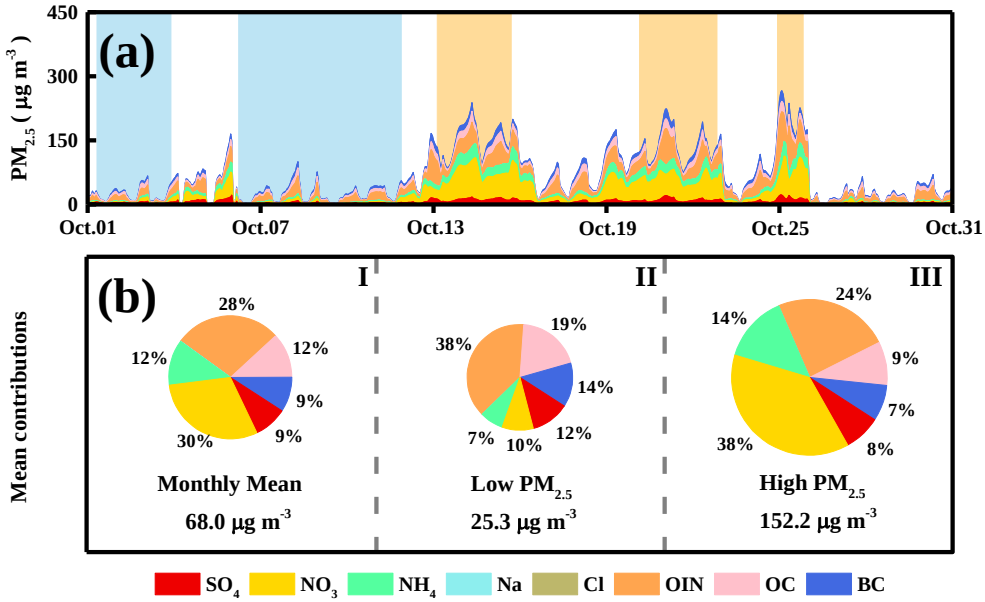

Figure R1. Time series (a) and mean contributions (b) of the simulated aerosol species at Xianghe station during Oct. 2018. I for the whole month; II for clean days (blue shaded parts in a); III for polluted days (yellow shaded parts in a).

In this study, MOSAIC-8bins was used as the aerosol chemistry mechanism. This mechanism includes eight aerosols species: Sulfate (SO_4), Nitrate (NO_3), Ammonium (NH_4), Sodium (Na), Chlorine (Cl), Organic Carbon (OC), Black Carbon (BC), and, Other Inorganics (OIN). Based on Fig. 2c in manuscript, concentrations of all the simulated aerosols species and their relative contributions to the total concentration of $PM_{2.5}$ at Xianghe station are shown in Fig. R1. During Oct. 2018, the mean concentration of $PM_{2.5}$ was 68.0 μg m^{-3} at Xianghe station. Among all the species, NO_3 and OIN contributed significantly which accounted for 30% and 28% to the total

concentration of $PM_{2.5}$; SO_4, NH_4, BC, and OC accounted for ~10%, respectively; Na and Cl showed few contributions during Oct. 2018. Under the "clean" condition (blue shaded parts in Fig. R1a and the pie chart II in Fig. R1b), the mean concentration of $PM_{2.5}$ decreased to 25.3 μg m^{-3} and OIN contributed (accounted for 38%) more than NO_3 did (accounted for 10%). On the contrary, OIN contributed (accounted for 24%) less than NO_3 did (accounted for 38%) when it was under the "polluted" condition (yellow shaded parts in Fig. R1a and the pie chart III in Fig. R1b).

Table R1. Refractive indexes of the aerosol species at each wave band in WRF-Chem model

wave band	300nm		400nm		600nm		999nm	
refr. index[a] / species	real[b]	imaginary[c]	real	imaginary	real	imaginary	real	imaginary
SO4	1.52	1.00×10^{-9}	1.52	1.00×10^{-9}	1.52	1.00×10^{-9}	1.52	1.75×10^{-9}
NO3	1.50	0.00	1.50	0.00	1.50	0.00	1.50	0.00
NH4	1.50	0.00	1.50	0.00	1.50	0.00	1.50	0.00
Na	1.51	8.66×10^{-7}	1.50	7.02×10^{-8}	1.50	1.18×10^{-8}	1.47	1.50×10^{-4}
Cl	1.51	8.66×10^{-7}	1.50	7.02×10^{-8}	1.50	1.18×10^{-8}	1.47	1.50×10^{-4}
OC	1.45	0.00	1.45	0.00	1.45	0.00	1.45	0.00
BC	1.85	0.71	1.85	0.71	1.85	0.71	1.85	0.71
OIN	1.55	3.00×10^{-3}	1.55	3.00×10^{-3}	1.55	3.00×10^{-3}	1.55	3.00×10^{-3}

[a] refr. index = refractive index; [b] real = real part; [c] imaginary = imaginary part

According to the source code of WRF-Chem model, the refractive index of each species was listed in Table R1. BC is a typical light-absorbing aerosol (Bond et al., 2004; 2013). Second to BC, OIN is also treated as light-absorbing aerosol since the imaginary part of which being larger than that of other species. The remaining species are treated as light-scattering aerosols. In order to showing the effects of the two types of aerosols on $J[NO_2]$, two more parallel experiments (Exp3 and Exp4) were designed: Exp3,

photolysis rate calculation without considering the optical properties of light-scattering aerosols; Exp4, photolysis rate calculation without considering the optical properties of light-absorbing aerosols. By comparing the results of Exp3 and Exp4 with the results of Exp1 respectively, the effects of light-absorbing aerosols and light-scattering aerosols on $J[NO_2]$ profile can be figured out.

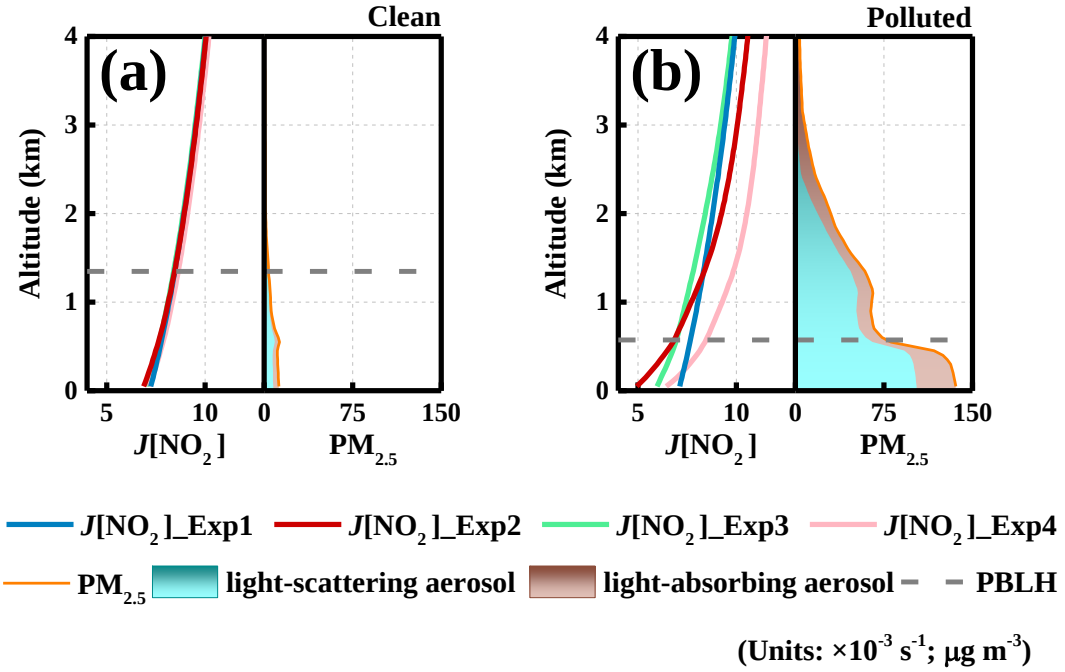

Figure R2. Mean profiles of $J[NO_2]$ and types of aerosols with diameter equal or less than 2.5 μg at 12:00 in clean days (a) and polluted days (b). Mean PBL height of the two kinds of days are also presented in (a) and (b), respectively.

Same as the data collection rule of Fig.3 in the manuscript but for the four experiments, the $J[NO_2]$ profiles under the low-level aerosol condition (clean) and high-level aerosol condition (polluted) at noon (12:00) are presented in Fig. R2. Correspondingly, the profiles of the two types of aerosols (cyan and brown shades) under clean and polluted conditions are also presented in Fig. R2a and R2b, respectively. Under clean condition (Fig. R2a), aerosols were at very low levels and didn't impact $J[NO_2]$ significantly. Consequently, the four profiles didn't show significant differences in vertical direction. Under polluted condition (Fig. R2b), the concentrations of $PM_{2.5}$

were at relatively high levels in the lowest 1.3 km ($PM_{2.5}$ with mean concentration of 90.0 μg m^{-3}; light-absorbing aerosols and light-scattering aerosols are 19.4 μg m^{-3} and 70.6 μg m^{-3}, respectively), especially in the PBL, where the mean concentration of $PM_{2.5}$ reached 123.1 μg m^{-3} (light-absorbing aerosols and light-scattering aerosols are 28.4 μg m^{-3} and 94.7 μg m^{-3}, respectively). Since light-absorbing effect of light-absorbing aerosols, the incident solar irradiance was attenuated (Ding et al., 2016; Gao et al., 2018) and $J[NO_2]$ profile ($J[NO_2]$_Exp3) decreased along with the vertical direction. For light-scattering aerosols, since high concentration being located in lower layer, the incident solar radiation could be scattered backward and enhance the shortwave radiation in higher layer. In this case, $J[NO_2]$ ($J[NO_2]$_Exp4) aloft was enhanced. However, the incident solar irradiance was attenuated at the layers near the surface which leading to the decrease in $J[NO_2]$ near the surface. Combining the effects of the two types of aerosols, the light extinction of aerosols on $J[NO_2]$ ($J[NO_2]$_Exp2) decreased at the lowest 1.3 km but enhanced above 1.3 km.

Unfortunately, since lacking of relevant observations of the aerosol species, concentrations of the simulated aerosols species could not be validated and this may cause uncertainties to the impacts of different types of aerosols on $J[NO_2]$ profiles. Thus, we just present these results and discussions in the response material. However, our validations on $PM_{2.5}$, $J[NO_2]$, and $J[O_3{}^1D]$ are acceptable which suggested that the results on the light extinction of aerosols on photolysis rates and its effect on ozone concentrations which we discussed in our study are meaningful. In addition, our results are consistent with results from other study (Dickerson et al., 1997) which also demonstrate the validity of the results we presented in the manuscript.

It should be noted that different contributions of aerosol species could impact photolysis rates differently. Aerosols species contributed very differently at different places. Figuring out the effects of aerosols on $J[NO_2]$ profiles over East China is an interesting topic which being worthy of further studying.

(3) Line 99, add a comma after “combustion”

Reply: Thanks, we have added a comma after “combustion”. Please check the detail in

the revised manuscript at line 101.

(4) Line 135, add a comma after “episodes”

Reply: Thanks, we have added a comma after “episodes”. Please check the detail in the revised manuscript at line 138.

(5) Variables in Table 2 need to be added with units.

Reply: Thank you very much. Units of all the variables in Table 2 have been added. Details could be checked in the Table 2 in the revised manuscript.

(6) Caption of figure 6 needs to be updated. “CASE1” and “CASE2” should be replaced by “Exp1” and “Exp2”.

Reply: Thank you for the comment. We have updated the caption of figure 6. “CASE1” and “CASE2” have been replace by “Exp1” and “Exp2”. Please check the new caption of figure 6 in the revised manuscript.

Reference

Bond, T. C., Streets, D. G., Yarber, K. F., Nelson, S. M., Woo, J. H., and Klimont, Z.: A technology-based global inventory of black and organic carbon emissions from combustion, J. Geophys. Res., 109, D14203, https://doi.org/doi:10.1029/2003JD003697, 2004.

Bond, T. C., Doherty, S. J., Fahey, D. W., Forster, P. M., Berntsen, T., DeAngelo, B. J., Flanner, M. G., Ghan, S., Karcher, B., Koch, D., Kinne, S., Kondo, Y., Quinn, P. K., Sarofim, M. C., Schultz, M. G., Schulz, M., Venkataraman, C., Zhang, H., Zhang, S., Bellouin, N., Guttikunda, S. K., Hopke, P. K., Jacobson, M. Z., Kaiser, J. W., Klimont, Z., Lohmann, U., Schwarz, J. P., Shindell, D., Storlvmo, T., Warren, S. G., and Zender, C. S.: Bounding the role of black carbon in the climate system: A scientific assessment, J. Geophys. Res.: Atmos., 118, 5380–5552, https://doi.org/doi:10.1002/jgrd.50171, 2013.

Ding, A. J., Huang, X., Nie, W., Sun, J. N., Kerminen, V. M., Petaja, T., Su, H., Cheng, Y. F., Yang, X. Q., Wang, M. H., Chi, X. G., Wang, J. P., Virkkula, A., Guo, W. D., Yuan, J., Wang, S. Y., Zhang, R. J., Wu, Y. F., Song, Y., Zhu, T., Zilitinkevich, S., Kulmala, M., and Fu, C. B.: Enhanced haze pollution by black carbon in megacities in China, Geophys. Res. Lett., 43, 2873-2879, https://doi.org/10.1002/2016GL067745, 2016.

Dickerson, R. R., Kondragunta, S., Stenchikov, G., Civerolo, K. L., Doddridge, B. G., and Holben, B. N.: The impact of aerosols on solar ultraviolet radiation and photochemical smog, Science, 278, 827-830, https://doi.org/10.1126/science.278.5339.827, 1997.

Gao, J. H., Zhu, B., Xiao, H., Kang, H. Q., Pan, C., Wang, D. D., and Wang, H. L.: Effects of black carbon and boundary layer interaction on surface ozone in Nanjing, China, Atmos. Chem. Phys., 18, 7081-7094, https://doi.org/10.5194/acp-18-7081-2018, 2018.

Dear editor and referee#2,

Thank you very much for your time and attentions on this work. The comments and suggestions are very useful to improve our manuscript. Following is a point-by-point response to referee #2's comments. Texts in black are the comments, those in blue are our responses. All the line numbers mentioned in responses are referred to the manuscript with changes marked.

We hope that you will find the changes satisfactory and we are looking forward to hearing from you soon.

I have one major concern regarding the mass balance technique, its description, and the interpretation of the results. Any balance equation inevitably has the residual term, which includes "other" processes (uncategorized) and the numerical error term. During the analysis, one has to show that the specified term (for example, net chemical production or vertical entrainment) are much larger than this residual term.
Could authors, please, add the mass balance equation and the short description (possibly to the supplementary), which explicitly states all of the terms and address the following questions:

(1) How well does the mass balance equation balance? What is the magnitude of the "numerical error" term compared to the other terms? Often, this term has the same order of magnitude. In this study, however, the agreement is exact (for example, Table 3 and 4)

Reply: Thank you for your comment. In WRF-Chem model, chemical species undergo the physical and chemical processes that are presented in Fig. R1. The contribution of each process at each time step is represented by the difference between the concentration after the process calculation (C^{new}) and the concentration before the

process calculation (C^{old}).

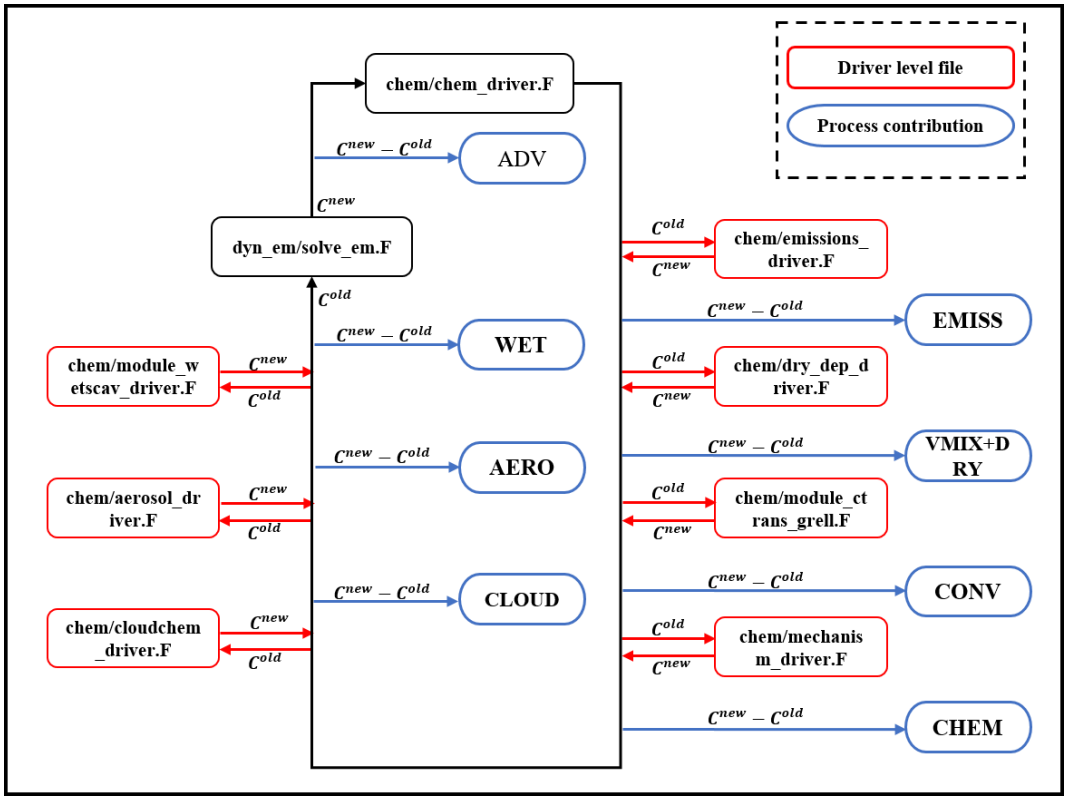

Figure R1: Schematic showing the calculation flow of chemical species in the WRF-Chem model.

In this case, for any chemical species at any grid, the change of concentration (ΔC) at each time step equals to:

$$\Delta C = ADV + EMISS + VMIX + DRY + CONV + CHEM + CLOUD + AERO + WET$$

Among them, ADV is the contribution from advection; EMISS is the contribution from direct emission; VMIX is the contribution from vertical mixing process; DRY is the contribution from dry deposition; CONV is the contribution from convection; CHEM is the contribution from gas-phase chemistry; CLOUD is the contribution from cloud chemistry; AERO is the contribution from aerosol chemistry; WET is the contribution

from wet deposition. For ozone, some of the terms don't contribute the change of ozone (ΔOzone). As a typical secondary pollution, there is no direct emission of ozone in the model and EMISS is 0.0. MOSAIC was used as aerosol chemistry mechanism in this study. This mechanism involves processes such as heterogeneous reactions, gas-particle mass transfer process, nucleation and coagulation (Zaveri et al., 2008). However, ozone doesn't participate in the relevant calculations which means AERO is 0.0. Same as aerosol chemistry, ozone also doesn't participate in the calculation of cloud chemistry and the CLOUD is 0.0. Because we selected the simulated data which was under the clear sky conditions, there was no contribution from wet deposition (WET=0.0). In this case, for ΔOzone, the mass balance equation can be simplified to:

$$\Delta Ozone = ADV + VMIX + DRY + CHEM + CONV$$

Since occurring on the ground level, DRY only shows contribution in the first layer in the model domain. Thus, the mass balance equation of ΔOzone at any grid and at each time step can be shown as:

$$\Delta Ozone = \begin{cases} ADV + CHEM + VMIX + CONV + DRY & in\ 1^{st}\ layer \\ ADV + CHEM + VMIX + CONV & above\ 1^{st}\ layer \end{cases}$$

The original WRF-Chem model has provided some processes diagnostic variables (names of these variables are advz_o3, advh_o3, chem_o3, vmix_o3, conv_o3) to show the contributions of the primary processes to ozone concentrations. According to the original model code, each process diagnostic variable is the accumulation of the difference of the ozone concentration between after and before the corresponding process calculation at each time step. The variables advh_o3 and advz_o3 represent the contributions from horizontal advection and zonal advection. And the contribution of ADV is the sum of advh_o3 and advz_o3 (ADV=advh_o3+advz_o3). The variable chem_o3 represents the contribution of CHEM. Dry deposition occurred at surface which is located in the first layer in the model domain. It is calculated together with

vertical mixing process in the subroutine vertmx (chem/module_vertmx_wrf.F) which belongs to the module of dry_dep_driver (chem/dry_dep_driver.F). Thus, in the first layer, the variable vmix_o3 is the sum contribution of VMIX and DRY. And above the first layer, vmix_o3 equals to the contribution of VMIX. In order to discussing processes contributions on surface ozone more clearly, the contributions of DRY and VMIX have been separated from the vmix_o3 (method can be check in the reply of question 2 and the supplementary material) and we ran the two experiments again. In addition, conv_o3 represents the contribution of CONV which may impact ozone concentration when it occurred in the atmosphere. However, in this study, contribution of CONV was 0.0 during the periods we discussed and was not mentioned in our manuscript. The description on mass balance for WRF-Chem model has been presented in the supplementary material.

From the above, it's clear that ΔOzone at any grid and at any time step equal to the sum of the processes contributions mentioned in the manuscript and it also suggested that the mass balance of our simulated results kept well. Because of the calculation method of the processes contributions, the numerical error between the change of ozone concentration and processes contributions is relatively small. However, there are still some numerical error caused by the calculation accuracy in our results. Taking the results in Table 3 in manuscript as an example (shown in Table R1):

Table R1. Detail information for Table 3 in the manuscript.

ΔO_3^{at} 14:00	$\sum_{i=8:00}^{14:00} CHEM\_DIF_i$	$\sum_{i=8:00}^{14:00} VMIX\_DIF_i$	$\sum_{i=8:00}^{14:00} DRY\_DIF_i$	$\sum_{i=8:00}^{14:00} ADV\_DIF_i$	$\sum_{i=8:00}^{14:00} NET\_DIF_i$
-11.70516 ppb	-44.28622 ppb	12.00781 ppb	19.58756 ppb	0.91944 ppb	-11.77141 ppb

As shown in Table R1, at 14:00, the difference of ozone between Exp1 and Exp2 (Exp2-Exp1) is -11.70516 ppb. The accumulated tendency of the change in each process between Exp1 and Exp2 from 08:00 to 14:00 is also listed in Table R1. $\sum_{08:00}^{14:00} CHEM\_DIF$, $\sum_{08:00}^{14:00} VMIX\_DIF$, $\sum_{08:00}^{14:00} DRY\_DIF$, $\sum_{08:00}^{14:00} ADV\_DIF$ and are -44.28622 ppb, 12.00781 ppb, 19.58756 ppb, and 0.91944 ppb, respectively. And their

sum ($\sum_{08:00}^{14:00} NET\_DIF$) is -11.77141 ppb.

$$\sum_{08:00}^{14:00} NET\_DIF = \sum_{08:00}^{14:00} ADV\_DIF + \sum_{08:00}^{14:00} VMIX\_DIF + \sum_{08:00}^{14:00} CHEM\_DIF + \sum_{08:00}^{14:00} DRY\_DIF$$

We can see that the bias between $\Delta O_3^{at\ 14:00}$ and $\sum_{08:00}^{14:00} NET\_DIF$ is 0.06625 ppb which is much less than other terms. In order to making the table clear, all data in table 3 reserved a decimal fraction and the bias became 0.1 ppb.

(2) Was the dry deposition taken into account? If it is incorporated into one of the three considered terms (CHEM, ADV, or VMIX), then it has to be extracted and presented separately, or the terms should be renamed (for example, CHEM+DEP)

Reply: Thank you for your comment. Dry deposition was taken into account. In previous version of this manuscript, we used result of vmix_o3 to represent the contribution of VMIX. Since the dry deposition and vertical mixing being calculated together in WRF-Chem model, vmix_o3 in the first layer actually contained the contributions of DRY and VMIX. Thus, the VMIX mentioned in section 3.3.1 in previous version of the manuscript contained the contribution of DRY. In order to making the discussion of process analysis on surface ozone more clearly, we followed the comment and separated the contributions of DRY and VMIX from vmix_o3.

It has been known that, pressure and temperature are not changed when doing the dry deposition calculation. Thus, the contribution of DRY to ozone (C_{O3}) at each time step (dt) can be calculated as:

$$DRY = C_{O3} * dvel * dt/dz$$

In which, dvel is the dry deposition velocity of ozone and dz is the height of the grid. And the contribution of VMIX in the first layer at each time step equals to:

$$VMIX = vmix\_o3 - DRY$$

Relevant modifications of the code were added into WRF-Chem model. And we ran the two experiments again. The results showed that, since the decrease of surface ozone, the dry deposition of ozone was weakened which leading to the change in DRY

increased during daytime. In addition, the change in VMIX was increased which is due to the enhancement of the vertical mixing process. The increases in DRY and VMIX partly counteracted the reduction in CHEM. Relevant discussion in section 3.3.1, Fig. 5, and Table 3 have been revised, please check the details in the revised manuscript.

(3) How was the NET term obtained (for example, in figure 5)? Is it merely a sum of ADV+VMIX+CHEM terms or is obtained directly from the separate WRF-Chem output variable, which represented the d[X]/dt?

Reply: The NET contribution is the sum of all the processes contributions.

For any grid in the first layer:

$$\mathrm{NET} = \mathrm{ADV} + \mathrm{CHEM} + \mathrm{DRY} + \mathrm{VMIX}$$

For any grid above the first layer:

$$\mathrm{NET} = \mathrm{ADV} + \mathrm{CHEM} + \mathrm{VMIX}$$

In the manuscript, we used NET to represent the hourly net contribution from all the mentioned processes.

(4) Given the reasonable model-observation comparison statistics, net chemical production (CHEM) and vertical mixing (VMIX) are likely the only major drivers, but the scientific analysis has to be rigorous.

My minor concern is related to the effect of aerosols on PBL height. In section 3.2 and Figure 3, the authors contrast the clean and polluted cases. The impact of the aerosols on PBL height is vivid (Figure 3, polluted case). However, no discussion on the aerosols properties or the effect of the collapsed PBL is offered. I think that manuscript will improve if authors describe in the text the composition of the aerosols (primary type) and the absorption properties (single scattering albedo). Additional, considering that tracers are well mixed within the PBL, the PBL reduction by a factor of 2 translates roughly in a two-times increase in tracer concentrations. What role does the PBL collapse play in the adjustment of the surface ozone concentration compared to the aerosols effect on photolysis and vertical entrainment?

Reply: Thank you for your comment. Based on the optical properties of aerosols, they

can be classified into light-scattering aerosols and light-absorbing aerosols. Before talking about the comprehensive effects of aerosols on $J[NO_2]$, it's necessary to present the effects of light-scattering aerosols and light-absorbing aerosols on $J[NO_2]$, respectively.

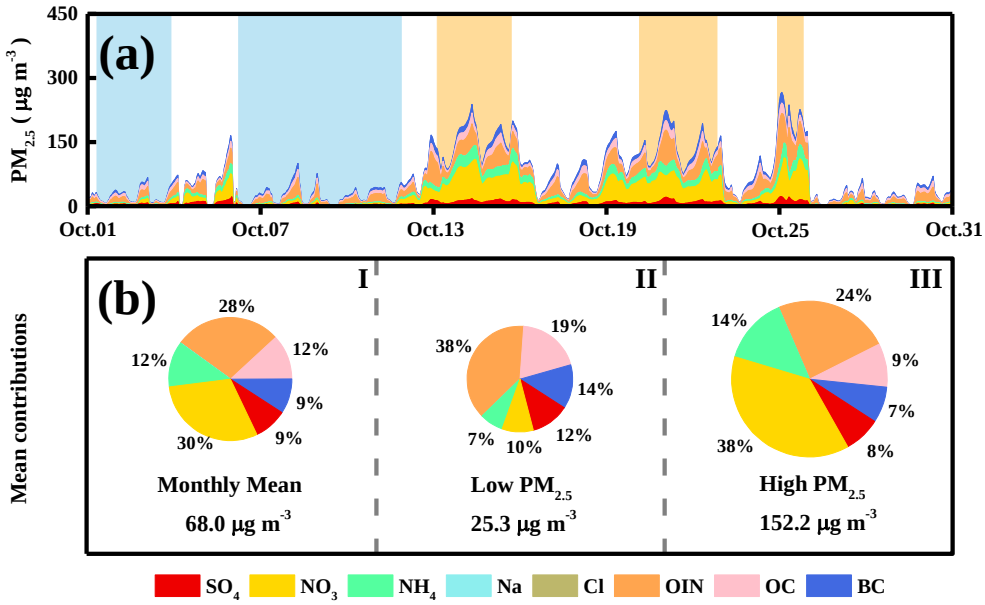

Figure R2. Time series (a) and mean contributions (b) of the simulated aerosol species at Xianghe station during Oct. 2018. I for the whole month; II for clean days (blue shaded parts in a); III for polluted days (yellow shaded parts in a).

In this study, MOSAIC-8bins was used as the aerosol chemistry mechanism. This mechanism includes eight aerosols species: Sulfate (SO_4), Nitrate (NO_3), Ammonium (NH_4), Sodium (Na), Chlorine (Cl), Organic Carbon (OC), Black Carbon (BC), and, Other Inorganics (OIN). Based on Fig. 2c in manuscript, concentrations of all the simulated aerosols species and their relative contributions to the total concentration of $PM_{2.5}$ at Xianghe station are shown in Fig. R2. During Oct. 2018, the mean concentration of $PM_{2.5}$ was 68.0 μg m^{-3} at Xianghe station. Among all the species, NO_3 and OIN contributed significantly which accounted for 30% and 28% to the total concentration of $PM_{2.5}$; SO_4, NH_4, BC, and OC accounted for ~10%, respectively; Na and Cl showed few contributions during Oct. 2018. Under the "clean" condition (blue shaded parts in Fig. R2a and the pie chart II in Fig. R2b), the mean concentration of

$PM_{2.5}$ decreased to 25.3 μg m^{-3} and OIN contributed (accounted for 38%) more than NO_3 did (accounted for 10%). On the contrary, OIN contributed (accounted for 24%) less than NO_3 did (accounted for 38%) when it was under the "polluted" condition (yellow shaded parts in Fig. R2a and the pie chart III in Fig. R2b).

Table R2. Refractive indexes of the aerosol species at each wave band in WRF-Chem model

wave band	300nm		400nm		600nm		999nm	
refr. index[a] / species	real[b]	imaginary[c]	real	imaginary	real	imaginary	real	imaginary
SO4	1.52	1.00×10^{-9}	1.52	1.00×10^{-9}	1.52	1.00×10^{-9}	1.52	1.75×10^{-9}
NO3	1.50	0.00	1.50	0.00	1.50	0.00	1.50	0.00
NH4	1.50	0.00	1.50	0.00	1.50	0.00	1.50	0.00
Na	1.51	8.66×10^{-7}	1.50	7.02×10^{-8}	1.50	1.18×10^{-8}	1.47	1.50×10^{-4}
Cl	1.51	8.66×10^{-7}	1.50	7.02×10^{-8}	1.50	1.18×10^{-8}	1.47	1.50×10^{-4}
OC	1.45	0.00	1.45	0.00	1.45	0.00	1.45	0.00
BC	1.85	0.71	1.85	0.71	1.85	0.71	1.85	0.71
OIN	1.55	3.00×10^{-3}	1.55	3.00×10^{-3}	1.55	3.00×10^{-3}	1.55	3.00×10^{-3}

[a] refr. index = refractive index; [b] real = real part; [c] imaginary = imaginary part

According to the source code of WRF-Chem model, the refractive index of each species was listed in Table R2. BC is a typical light-absorbing aerosol (Bond et al., 2004; 2013). Second to BC, OIN is also treated as light-absorbing aerosol since the imaginary part of which being larger than that of other species. The remaining species are treated as light-scattering aerosols. In order to showing the effects of the two types of aerosols on $J[NO_2]$, two more parallel experiments (Exp3 and Exp4) were designed: Exp3, photolysis rate calculation without considering the optical properties of light-scattering aerosols; Exp4, photolysis rate calculation without considering the optical properties of light-absorbing aerosols. By comparing the results of Exp3 and Exp4 with the results

of Exp1 respectively, the effects of light-absorbing aerosols and light-scattering aerosols on $J[NO_2]$ profile can be figured out.

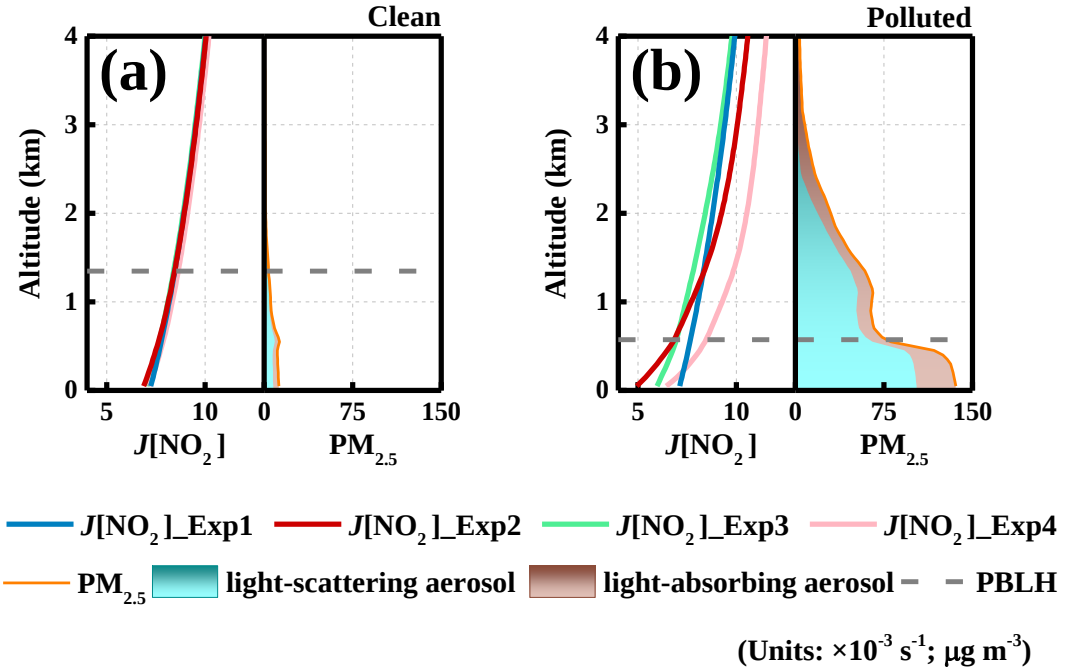

Figure R3. Mean profiles of $J[NO_2]$ and types of aerosols with diameter equal or less than 2.5 μg at 12:00 in clean days (a) and polluted days (b). Mean PBL height of the two kinds of days are also presented in (a) and (b), respectively.

Same as the data collection rule of Fig.3 in the manuscript but for the four experiments, the $J[NO_2]$ profiles under the low-level aerosol condition (clean) and high-level aerosol condition (polluted) at noon (12:00) are presented in Fig. R3. Correspondingly, the profiles of the two types of aerosols (cyan and brown shades) under clean and polluted conditions are also presented in Fig. R3a and R3b, respectively. Under clean condition (Fig. R3a), aerosols were at very low levels and didn't impact $J[NO_2]$ significantly. Consequently, the four profiles didn't show significant differences in vertical direction. Under polluted condition (Fig. R3b), the concentrations of $PM_{2.5}$ were at relatively high levels in the lowest 1.3 km ($PM_{2.5}$ with mean concentration of 90.0 μg m^{-3}; light-absorbing aerosols and light-scattering aerosols are 19.4 μg m^{-3} and 70.6 μg m^{-3}, respectively), especially in the PBL, where the mean concentration of

$PM_{2.5}$ reached 123.1 μg m^{-3} (light-absorbing aerosols and light-scattering aerosols are 28.4 μg m^{-3} and 94.7 μg m^{-3}, respectively). Since light-absorbing effect of light-absorbing aerosols, the incident solar irradiance was attenuated (Ding et al., 2016; Gao et al., 2018) and $J[NO_2]$ profile ($J[NO_2]$_Exp3) decreased along with the vertical direction. For light-scattering aerosols, since high concentration being located in lower layer, the incident solar radiation could be scattered backward and enhance the shortwave radiation in higher layer. In this case, $J[NO_2]$ ($J[NO_2]$_Exp4) aloft was enhanced. However, the incident solar irradiance was attenuated at the layers near the surface which leading to the decrease in $J[NO_2]$ near the surface. Combining the effects of the two types of aerosols, the light extinction of aerosols on $J[NO_2]$ ($J[NO_2]$_Exp2) decreased at the lowest 1.3 km but enhanced above 1.3 km.

Unfortunately, since lacking of relevant observations of the aerosol species, concentrations of the simulated aerosols species could not be validated and this may cause some uncertainties to the impacts of different types of aerosols on $J[NO_2]$ profiles. Thus, we just present these results and discussions in the response material. However, our validations on $PM_{2.5}$, $J[NO_2]$, and $J[O_3{}^1D]$ are acceptable which suggested that the results on the light extinction of aerosols on photolysis rates and its effect on ozone concentrations which we discussed in our study are meaningful. In addition, our results are consistent with that from other study (Dickerson et al., 1997) which also demonstrate the validity of the results we presented in the manuscript.

It should be noted that different contributions of aerosol species could impact photolysis rates differently. Aerosols species contributed very differently at different places. Figuring out the effects of aerosols on $J[NO_2]$ profiles over East China is an interesting topic which being worthy of further studying.

The light extinction of aerosols can influence ozone not only via affecting photolysis rate, but also via suppressing the PBL. In this study, we mainly focus on the impact of light extinction of aerosols on photolysis rate and how this impact influence ozone. The difference between the two experiments we designed is just at whether taking optical properties of the aerosols into the calculation of photolysis rate. And other

parts of the model system are not modified. There were not significant differences in concentrations of $PM_{2.5}$ and the PBLHs between Exp1 and Exp2 (Fig. R4), especially the PBLHs from Exp1 and Exp2 are almost the same, which suggested that the effects of the collapsed PBL on ozone induced by aerosols could not be shown in this study.

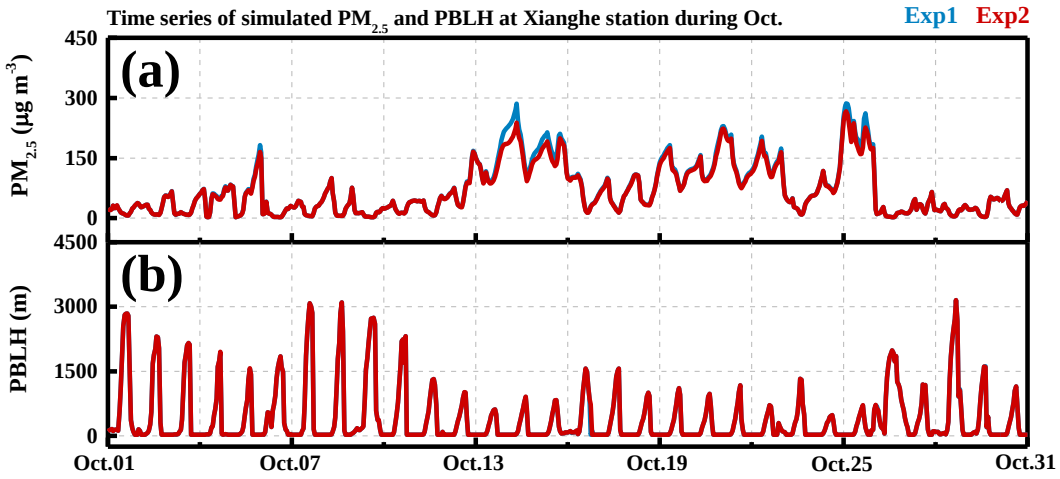

Figure R4. Time series of the simulated $PM_{2.5}$ (a) and PBLH (b) from Exp1 and Exp2 at Xianghe station during Oct. 2018.

However, this comment is very meaningful. Effects of PBL, especially the effects of the interaction between PBL and aerosols, is an important impact on ozone which we have discussed in another paper (Gao et al., 2018). The suppression of PBL induced by the light extinction of aerosol can weakened the entrainment of turbulence aloft which leading to less ozone with high concentrations being transported down to the surface. Furthermore, the suppression of PBL can confine more ozone precursors in the PBL which may enhance the contribution of CHEM. However, when considering the decrease of photolysis rate induced by the light extinction of aerosol simultaneously, the contribution of CHEM may change differently and the change of ozone concentration may be different too. These multiple influence paths on ozone remind us that more clearly study on each impact first is very necessary. And this is also the purpose for us to conduct this study. We believe that, on the basis of this study, the effect of the interaction between PBL and aerosols on ozone will be studied more clearly in future work. And again, we really thank you for your enlightening comments.

Technical corrections

(1) References should be formatted appropriately and numbered.

Reply: Thank you for your comment. According to the format requirements of the references (https://www.atmospheric-chemistry-and-physics.net/for_authors/manuscript_preparation.html), we have reformatted all the references. However, the requirements and the format template don't list the references with numbers. Thus, numbers to references were not listed but we believe that the new reference list has become clearer than the previous version. Please check the new reference list in the revised manuscript.

(2) Please, add units to Table 2.

Reply: Thank you for your comment. Units of all the variables have been added in Table 2. Please check the new Table 2 in the revised manuscript.

(3) Line 224. Delete "which showed that ozone stopped decreasing"

Reply: Thank you very much. We follow this comment. And "which showed that ozone stopped decreasing" has been deleted. Please check the detail in the revised manuscript at lines 246~247.

(4) Figure 6, Please, update the caption, remove the CASE* and explain that data was spatially sampled and represent four cities.

Reply: Thank you for your comment. We have updated the caption of Fig. 6. Some important information has been added in it. Please check the new caption of Fig. 6 in the revised manuscript.

Reference

Bond, T. C., Streets, D. G., Yarber, K. F., Nelson, S. M., Woo, J. H., and Klimont, Z.: A technology-based global inventory of black and organic carbon emissions from

combustion, J. Geophys. Res., 109, D14203, https://doi.org/doi:10.1029/2003JD003697, 2004.

Bond, T. C., Doherty, S. J., Fahey, D. W., Forster, P. M., Berntsen, T., DeAngelo, B. J., Flanner, M. G., Ghan, S., Karcher, B., Koch, D., Kinne, S., Kondo, Y., Quinn, P. K., Sarofim, M. C., Schultz, M. G., Schulz, M., Venkataraman, C., Zhang, H., Zhang, S., Bellouin, N., Guttikunda, S. K., Hopke, P. K., Jacobson, M. Z., Kaiser, J. W., Klimont, Z., Lohmann, U., Schwarz, J. P., Shindell, D., Storlvmo, T., Warren, S. G., and Zender, C. S.: Bounding the role of black carbon in the climate system: A scientific assessment, J. Geophys. Res.: Atmos., 118, 5380–5552, https://doi.org/doi:10.1002/jgrd.50171, 2013.

Dickerson, R. R., Kondragunta, S., Stenchikov, G., Civerolo, K. L., Doddridge, B. G., and Holben, B. N.: The impact of aerosols on solar ultraviolet radiation and photochemical smog, Science, 278, 827-830, https://doi.org/10.1126/science.278.5339.827, 1997.

Ding, A. J., Huang, X., Nie, W., Sun, J. N., Kerminen, V. M., Petaja, T., Su, H., Cheng, Y. F., Yang, X. Q., Wang, M. H., Chi, X. G., Wang, J. P., Virkkula, A., Guo, W. D., Yuan, J., Wang, S. Y., Zhang, R. J., Wu, Y. F., Song, Y., Zhu, T., Zilitinkevich, S., Kulmala, M., and Fu, C. B.: Enhanced haze pollution by black carbon in megacities in China, Geophys. Res. Lett., 43, 2873-2879, https://doi.org/10.1002/2016GL067745, 2016.

Gao, J. H., Zhu, B., Xiao, H., Kang, H. Q., Pan, C., Wang, D. D., and Wang, H. L.: Effects of black carbon and boundary layer interaction on surface ozone in Nanjing, China, Atmos. Chem. Phys., 18, 7081-7094, https://doi.org/10.5194/acp-18-7081-2018, 2018.

Zaveri, R. A., Easter, R. C., Fast, J. D., and Peters, L. K.: Model for simulating aerosol interactions and chemistry (MOSAIC), J. Geophys. Res.-Atmos., 113, D13204, https://doi.org/10.1029/2007jd008782, 2008.

What have we missed when studying the impact of aerosols on surface ozone via changing photolysis rates?

Jinhui Gao[1,2], Ying Li[1], Bin Zhu[3,4], Bo Hu[5], Lili Wang [5], Fangwen Bao[1,2]

[1]Department of Ocean Science and Engineering, Southern University of Science and Technology, Shenzhen, China
[2]School of Earth and Space Sciences, University of Science and Technology of China, Hefei, China
[3]Collaborative Innovation Center on Forecast and Evaluation of Meteorological Disasters, Nanjing University of Information Science and Technology, Nanjing, China
[4]Key Laboratory of Aerosol-Cloud-Precipitation of China Meteorological Administration, Nanjing University of Information Science and Technology, Nanjing, China
[5]State Key Laboratory of Atmosphere Boundary Layer Physics and Atmospheric Chemistry (LAPC), Institute of Atmospheric Physics, Chinese Academy of Sciences, Beijing, China

Correspondence to: Ying Li (liy66@sustech.edu.cn)

Abstract. Previous studies have emphasized that the decrease in photolysis rate at the surface induced by the light extinction of aerosols could weaken ozone photochemistry and then reduce surface ozone. However, quantitative studies have shown that weakened photochemistry leads to a much greater reduction in the net chemical production of ozone, which does not match the reduction in surface ozone. This suggested that in addition to photochemistry, some other physical processes related to the variation of ozone should also be considered. In this study, the Weather Research and Forecasting with Chemistry (WRF-Chem) model coupled with the ozone source apportionment method was applied to determine the mechanism of ozone reduction induced by aerosols over Central East China (CEC). Our results showed that weakened ozone photochemistry led to a significant reduction in ozone net chemical production, which occurred not only at the surface but also within the lowest several hundred meters in the planetary boundary layer (PBL). Meanwhile, a larger ozone gradient was formed in vertical direction, which led to the high concentrations of ozone aloft being entrained by turbulence from the top of the PBL to the surface and partly counteracting the reduction in surface ozone. In addition, contribution from dry deposition was weakened due to the decrease in surface ozone concentration. The reduction in the ozone's sink also slowing down the tendency of the decrease in surface ozone. ~~ozone~~ Ozone in the upper layer of the PBL was also reduced, which was ~~also~~ induced by much ozone aloft being entrained downward. Therefore, by affecting the photolysis rate, the impact of aerosols was a reduction in ozone not only at the surface but also throughout the entire PBL during the daytime over the CEC in this study. The ozone source apportionment results showed that 41.4%–66.3% of the reduction in surface ozone came from local and adjacent source regions, which suggested that the impact of aerosols on ozone from local and adjacent regions was more significant than that from long-distance regions. The results also suggested that while controlling the concentration of aerosols, simultaneously controlling ozone precursors from local and adjacent source regions is an effective way to suppress the increase in surface ozone over CEC at present.

1 Introduction

Ozone in the troposphere, especially in the planetary boundary layer (PBL), is a well-known secondary air pollutant that is seriously harmful to human health and vegetation (Haagen-Smit and Fox, 1954). As an important source of tropospheric ozone, the photochemical production of ozone is significantly affected by ozone precursors (i.e., NO_x and VOCs) and photolysis rates, and the latter is determined by the intensity of solar irradiance (Crutzen, 1973; Monks et al., 2015). Aerosols in the troposphere, which are another well-known air pollutant, can influence ozone levels through multiple pathways, for example, modulating temperature (Hansen et al., 1997), light extinction (Dickerson et al., 1997; Gao et al., 2018a), scavenging hydroperoxy (HO_2) and NO_x radicals (Li et al., 2019a, b). The light extinction of aerosols can reduce ozone net production (the sum of ozone chemical production and loss) at the surface by reducing the photolysis rate (i.e., $J[NO_2]$ and $J[O_3{}^1D]$; Dickerson et al., 1997), which we refer to as the "direct impact". Alternatively, light extinction caused by absorbing aerosols (i.e., black carbon) can suppress the development of the PBL (Ding et al., 2016) and then influence the surface ozone during the daytime (Gao et al., 2018a), which we refer to as the "indirect impact". Studies on the "direct impact" have been conducted in many places around the world (Jacobson, 1998; Castro et al., 2001; Li et al., 2005; Li et al., 2011a), especially in highly polluted regions such as "Beijing-Hebei-Tianjin" region in China (Bian et al., 2007; Deng et al., 2012; Xing et al., 2017); however, the mechanism of the "direct impact" still has not been fully explained.

Quantitative studies have suggested that, because of the impact of aerosols via affecting photolysis rates, 2%–17% of surface ozone decreased (Jacobson, 1998; Li et al., 2011b; Wang et al., 2016). However, these studies also showed that ozone net production decreased much more (Cai et al., 2013; Wang et al., 2019), which did not match the magnitude of the reduction in surface ozone. For example, a modeling study conducted by Li et al. (2011b) showed that the average reduction in surface ozone over Central East China (CEC) was -5.4 ppb, whereas the average reduction in ozone net production was -10.5 ppb. The difference between the two reductions indicates that, in addition to ozone photochemistry, there must be other ozone-related physical processes influenced by the reduction in photolysis rate induced by aerosols. However, pertinent studies are still lacking.

At present, air pollution in China is characterized by the "air pollution complex", which shows both aerosols (especially fine particulate matter $PM_{2.5}$) and ozone pollution issues in the atmosphere (Shao et al., 2006; Li et al., 2017b). With a series of stringent air pollution control policies conducted, the concentrations of aerosols have decreased in the past a few years (Wang et al., 2017); in contrast, the concentrations of ozone in China increased, especially in CEC (Reports on the State of the Environment in China, http://english.mee.gov.cn/Resources/Reports/soe/). Studies have suggested that the extensive reduction in aerosols may cause a potential risk of surface ozone enhancement (Anger et al., 2016; Wang et al., 2016). In this case, fully understanding and quantifying the impacts of aerosols on ozone is helpful for providing more reasonable advice for air quality protection policies in China.

In this study, the fully coupled "online" model system, Weather Research and Forecasting with Chemistry (WRF-Chem) model, was applied to simulate air pollutants over CEC in October 2018. The impact of aerosols on ozone via influencing the

photolysis rate was quantitatively studied by using process analysis, through a comparison between control and sensitivity simulations. In addition, with the application of the ozone source apportionment method (Gao et al., 2016; 2017) we developed and coupled with the WRF-Chem model system, the ozone contributions and their changes induced by aerosols over typical cities in CEC were also discussed quantitatively in this study. This paper is organized as follows. A description of the model setting, used data, and scenario design is presented in section 2. The results and discussion of the subject are presented in section 3. And finally, we end with the conclusions in section 4.

2 Methodology

2.1 Model configuration

The model system used in this study, the WRF-Chem model, is a fully coupled "online" 3-D Eulerian meteorological and chemical transport model that has been globally applied in air quality research (Tie et al., 2013; Zhang et al., 2014; Gao et al., 2018b; Hu et al., 2019). The version of the WRF-Chem model we used in this study is 3.9.1.1, and detailed introductions of the meteorological parts and chemical parts can be found in Skamarock et al. (2008) and Grell et al. (2005), respectively.

Regarding the simulation settings, two nested domains (Fig. 1) were set up with grid sizes of 122×122 and 150×150 at horizontal resolutions of 36 km and 12 km for the parent domain (D1) and nested domain (D2), respectively. D1 covered most parts of China and the surrounding areas and ocean, and D2 covered most parts of East China. The modeling results of D1 provided meteorological and chemical boundary conditions for the simulations of D2. For the vertical direction, 38 layers were set up from the surface up to a pressure limit at 50 hPa. It should be noted that 12 layers were located below the lowest 2 km, which is suitable for us to discuss the impacts of aerosols on ozone in the PBL. The Carbon Bond Mechanism Z (CBM-Z; Zaveri and Peters, 1999) was applied as the gas-phase chemical mechanism in this study. CBM-Z is the upgraded version of Carbon Bond IV (Gery et al., 1989), which includes 53 species with 133 reactions and extends the framework to function for larger spatial scale and longer time. Correspondingly, the Model for Simulating Aerosol Interactions and Chemistry with 8 bins (MOSAIC-8bins; Zaveri et al., 2008) was chosen as the aerosol chemistry mechanism. Other parameterization settings are listed in Table 1.

Since the light extinction of aerosols can impact ozone in two ways, it is necessary to distinguish the direct impact on ozone in this study. Thus, two parallel experiments were designed in this study: (1) photolysis rate calculation without the presence of aerosol optical properties (Exp1) and (2) photolysis rate calculation with considering the optical properties of all kinds of aerosols (Exp2). By comparing the results between Exp1 and Exp2, the impact of aerosols on ozone via influencing the photolysis rate can be determined. Both experiments started at 00:00 UTC on 29 September 2018 and ended at 00:00 UTC on 31 October 2018. The first two days were designated as the spin-up period.

2.2 Description of used data

Many kinds of data were used in this study. The initial and boundary meteorological and chemical conditions were provided by the National Centers for Environmental Prediction (NECP) final (FNL) operational global analysis data and outputs of the Community Atmosphere Model with Chemistry (CAM-chem; Lamarque et al., 2012). Regarding the emissions used in this study, anthropogenic emissions were provided by the Multi-resolution Emission Inventory for China (MEIC; http://www.meicmodel.org/). This inventory includes five anthropogenic sectors (industry, power plant, transportation, residential combustion, and agricultural activity), and each section contains both gas and aerosol species (SO_2, NO_x, NH_3, CO, VOCs, BC, OC, PM_{10}, and $PM_{2.5}$; Li et al., 2017a). Biogenic emissions were generated by using the Model of Emission of Gas and Aerosols from Nature (MEGAN; Guenther et al., 2006).

Meteorological observations (temperature, wind direction and wind speed) from 110 stations and air pollutants (ozone, NO_2 and $PM_{2.5}$) from 110 stations were collected to evaluate the model performance. The locations of the observation stations are presented in Fig. 1b. Hourly meteorological data were measured by the national surface observation network operated by the China Meteorological Administration (CMA). The hourly concentrations of air pollutants were measured and maintained by the China National Environmental Monitoring Center, and published online (http://113.108.142.147:20035/emcpublish). More information on the measurement of air pollutants can be seen in Wang et al. (2014b). In addition, relevant photolysis rates ~~the NO_2 photolysis rate~~ ($J[NO_2]$ and $J[O_3{}^1D]$) ~~was~~ were measured at a comprehensive observation station (116.95°E, 39.75°N; denoted with an up-ward triangle in Fig. 1b). The observation station, attached to the Institute of Atmospheric Physics (IAP) Chinese Academy of Sciences, is located in Xianghe, Hebei Province, approximately 65 km away from Beijing. The photolysis rates were measured by spectroradiometry technique (Hofzumahaus et al., 1999) with a measurement frequency of 10 s and in unit of s^{-1}. More information about the measurement technique is available in Hofzumahaus et al. (1999) and Bohn et al. (2004).

2.3 Source region settings for ozone source apportionment

Due to secondary pollutant properties, tropospheric ozone is highly dependent on the photochemical reactions of its precursors (NO_x and VOCs). In this study, an ozone source apportionment method was coupled into the WRF-Chem model. This approach, considering both NO_x-limited and VOC-limited conditions, is a mass balance technique that identifies the contributions from all geographic source regions to ozone in each grid or region in the model domain within one simulation. This method is similar to the Ozone Source Apportionment Technology (OSAT; Yarwood et al., 1996) which is coupled with the Comprehensive Air quality Model with extensions (CAMx; ENVIRON, 2011), with some modifications to suit the requirements of the WRF-Chem model. More information on the ozone source apportionment method can be found in Gao et al. (2016; 2017).

In this study, 20 geographic source regions were set up in the model domain. The North China Plain and eastern China are two economic hubs in China and suffered serious air pollutions in recent years (Wang et al., 2014a; 2014c; Ding et al., 2016;

Kang et al., 2019). As shown in Fig. 1, the two areas are separated into 10 source regions based on administrative divisions. Other provinces belonging to China and areas outside of China in the model domain are far from CEC but may also influence the air quality of CEC under favourable synoptic conditions. Thus, these regions were combined and defined as several source regions. Other details of the source regions are listed in Table S1, which can be seen in the supplementary material. In addition to the geographic source regions, chemical boundary condition provided by MOZART-4 outputs, named $O_{3\text{-Inflow}}$, was defined as an independent contribution, from which the air pollutants can flow into the model domain and impact ozone in CEC. The initial conditions of D1 (INIT1) and D2 (INIT2) were also settled as independent ozone contributions.

3 Results and discussion

3.1 Model validation

Although the WRF-Chem model has been widely used in air quality research, the performance varies dramatically when dealing with different domains, episodes, and parameterization settings. In this study, common model performance metrics (IOA: Index of Agreement; MB: mean bias; RMSE: root mean square error; MNB: mean normalized bias; MFB: mean fractional bias) were used to validate meteorological factors (T2: temperature at 2m above the surface; WS: wind speed at 10 m above the surface; WD: wind direction at 10 m above the surface) and air pollutants (ozone, NO_2 and $PM_{2.5}$). In addition, the observed time series of $J[NO_2]$ from Xianghe station was collected and used to validate the model performance for photolysis rate.

3.1.1 Model validation of meteorological and air quality simulations

For meteorological factors and air pollutants, observation data from more than 100 stations distributed in D2 (Fig. 1b) were collected. Considering the large data size, averaged model performance metrics are listed in Table 2. The benchmarks shown in brackets follow the recommended values suggested by Emery et al. (2001) and EPA (2005; 2007). In addition, the model performance of meteorological factors and air pollutants at each station is displayed by the Taylor diagram (Taylor, 2001; Gleckler et al., 2008) as shown in Figs. ~~S1~~ S2 and ~~S2~~S3, which are available in the supplementary material.

Regarding meteorological factors, T2 showed high values of the mean IOA, which was within the scope of its benchmark, indicating that the simulation agreed very well with the observations. The mean MB and RMSE of T2 were comparable with which in another modeling study (Hu et al., 2016) over the same region and during the same period. However, MB was slightly beyond the scope of its benchmark, which suggested a slight over-estimation of temperature. Simulations on wind speed showed satisfactory model performance since the values of IOA, MB and RMSE all met the criteria. Because of the vector nature of wind direction, the IOA of WD followed the calculation recommended by Kwok et al. (2010). The IOA of WD reached 0.89, which suggest a good agreement between the simulation and observation on wind direction. In addition, the MB was also within the benchmark, which also indicated the satisfactory model performance for wind direction.

For air pollutants, good agreement was found between the simulations and observations since the IOAs of ozone, NO_2 and $PM_{2.5}$ were 0.84, 0.73 and 0.74, respectively. The MNB of ozone was 0.16, which was slightly higher than the benchmark, while the MFB of $PM_{2.5}$ was within the scope of its benchmark. It should be noted that all of the model performance metrics of air pollutants were comparable with other modeling studies (Hu et al., 2016; Gao et al., 2018a) over CEC, which also indicated that our model performance for air pollutants was acceptable.

3.1.2 Model validation of $J[NO_2]$ and $J[O_3{}^1D]$

Figure 2a and 2b show~~s~~ the comparison of observed (dark gray dots) and predicted (red line, denotes results ~~$J[NO_2]$~~) in Exp2) $J[NO_2]$ and $J[O_3{}^1D]$ at Xianghe station. $J[NO_2]$ showed significant diurnal variations due to the strong dependence of photolysis on solar irradiance. Based on the comparison, the predicted $J[NO_2]$ agreed very well with the observed $J[NO_2]$ and can capture the variation pattern during the whole Oct. 2018. Comparing the simulated $J[NO_2]$ in Exp1 (blue line in Fig. 2a), the simulated $J[NO_2]$ in Exp2 agreed better with the observations than that in Exp1 (especially in the ~~during~~ "polluted" days with high concentrations of $PM_{2.5}$), which showed the reasonability of the calculations of the photolysis rate in Exp2 by considering the optical properties of aerosols. Similar to $J[NO_2]$, it also showed a good agreement between the observed $J[O_3{}^1D]$ and the predicted $J[O_3{}^1D]$. Since considering the impacts of aerosols on photolysis rates, the simulated $J[O_3{}^1D]$ in Exp2 more reasonably captured the variations of $J[O_3{}^1D]$. Especially during the "polluted" days, simulated $J[O_3{}^1D]$ in Exp2 decreased at daytime which was very close to the observations, however, the simulated $J[O_3{}^1D]$ in Exp1 didn't show this feature. The model performance metrics of Exp2 (presented in the top-right corner of Fig. 2a and Fig. 2b) also demonstrate the satisfactory model performance for $J[NO_2]$ and $J[O_3{}^1D]$. High values of IOAs (0.99 and 0.96) indicated excellent agreements of the time series patterns between observations and simulations. MBs (2.0×10^{-4}~~)~~ and ~~-~~0.47×10^{-6}~~-)~~ ~~was~~ were nearly one order of magnitude smaller than the average $J[NO_2]$ and $J[O_3{}^1D]$ (~~$\overline{OBS}$~~=1.6×10^{-3}~~)~~ and 0.31×10^{-5}~~)~~; in addition, the NMBs and NMEs ~~were~~ also ~~very small, which~~ indicated the satisfied agreements ~~a small bias~~ between observations and simulations.

3.2 Impact of aerosols on the photolysis rate

As shown in Fig. 2, when the concentrations of $PM_{2.5}$ (Fig. ~~2b~~2c) were low, for example, during the 1st–3rd and 6th–11th periods (the blue shaded parts), the surface $J[NO_2]$ in the~~se~~ two ~~cases~~ experiments were almost the same. However, when examining the polluted days (the yellow shaded parts), the surface $J[NO_2]$ decreased significantly due to the attenuation of incident solar irradiance induced by the light extinction of aerosols. It should also be noted that the light extinction of aerosols is not the only factor that affects the photolysis rate. Clouds can also affect the incident solar irradiance and significantly decrease the photolysis rate (Wild et al., 2000). That is why $J[NO_2]$ in Exp1 decreased during the daytime on the 15th Oct. However, the difference between Exp1 and Exp2 also reflected the impact of aerosols.

The impact of aerosols on the photolysis rate occurs not only at the surface but also along with the vertical direction. To investigate the aerosols' impact on the photolysis rate, the $J[NO_2]$ profiles under the low-level aerosol condition (clean) and

high-level aerosol condition (polluted) at noon (12:00) are compared in Fig. 3. The $J[NO_2]$ profiles with surface $PM_{2.5}$ concentrations lower than 35 μg m^{-3} were averaged to represent the $J[NO_2]$ profile under clean conditions (Fig. 3a). The $J[NO_2]$ profiles with surface $PM_{2.5}$ concentrations greater than 75 μg m^{-3} were averaged to represent the $J[NO_2]$ profile under polluted conditions (Fig. 3b). The referenced critical values of the surface $PM_{2.5}$ concentration (35 μg m^{-3} and 75 μg m^{-3}) were determined based on the national air quality standard (http://www.cnemc.cn/jcgf/dqhj/201706/W020181008687879597492.pdf). It should be noted that all the selected data was under clear sky conditions, which excludes the impacts of clouds on $J[NO_2]$.

Under clean conditions (Fig. 3a), $PM_{2.5}$ concentrations along with the vertical direction were low (with mean concentrations of 8.6 μg m^{-3} in the PBL and 1.0 μg m^{-3} above the PBL), which suggested that the impact of aerosols on the photolysis rate was small. Consequently, the two profiles did not show significant differences in the vertical direction. Under polluted conditions (Fig. 3b), the concentrations of $PM_{2.5}$ were at a relatively high level in the lowest 1.3 km (with mean value of 90.0 μg m^{-3}), especially in the PBL, where the mean concentration of $PM_{2.5}$ reached 123.1 μg m^{-3}. In this case, $J[NO_2]$ decreased with height in the lowest 1.3 km, which was due to the attenuation of incident solar irradiance induced by the light extinction of aerosols (Li et al., 2005; Li et al., 2011b). However, at altitude above 1.3 km with lower levels of $PM_{2.5}$, $J[NO_2]$ was enhanced, which could be due to the enhancement of light caused by the light-scattering effect of aerosols (i.e., sulfate aerosols) at the lower height. Our results regarding the changes in the $J[NO_2]$ profile caused by aerosols were consistent with the study of Dickerson et al. (1997).

3.3 Impact of aerosols on ozone via decreasing the photolysis rate

3.3.1 Changes in surface ozone induced by the decrease of photolysis rate

At the surface, the mean distributions of daytime $PM_{2.5}$ [from 08:00 to 17:00 local time (LT)] under polluted conditions over CEC are presented in Fig. 4a. Correspondingly, the change and relative change in ozone between Exp2 and Exp1 are illustrated in Fig. 4b and 4c, respectively.

High concentrations of $PM_{2.5}$ covered most of the Beijing-Tianjin-Hebei region and the northern Henan Province. In particular, cities with a large population, and large numbers of vehicles and industries, such as Beijing (BJ), Tianjin (TJ), Shijiazhuang (SJZ) and Zhengzhou (ZZ), suffered from more severe particle pollution (mean concentrations were 97.6, 99.8, 113.0 and 79.5 μg m^{-3} in BJ, TJ, SJZ, and ZZ, respectively). The distributions of surface ozone reduction (Fig. 4b and 4c) were similar to the distributions of $PM_{2.5}$ at the surface. More specifically, in the representative cities with severe particle pollution (BJ, TJ, SJZ and TJ), the mean reductions in surface ozone reached 10.6 ppb, 8.6 ppb, 8.2 ppb and 4.2 ppb, respectively, which accounted for 19.0 %, 19.4 %, 17.7 % and 7.9 % of the mean concentrations of surface ozone in these cities, respectively.

Chemical and physical processes analysis (Zhu et al., 2015; Gao et al., 2016) was implemented to discuss the mechanism of the surface ozone reduction induced by aerosols via influencing the photolysis rate in the four representative cities. The

following processes were considered: chemistry (CHEM, which is the sum of ozone chemical production and loss of ozone in atmosphere; this contribution is the same as the "ozone net production" which was mentioned in other studies), advection (ADV, which is caused by the transport effects of wind fields), and vertical mixing (VMIX, which is caused by turbulence in the PBL and is closely dependent on turbulence intensity and the vertical gradients of ozone). In addition, for surface ozone, the contribution of dry deposition (DRY, which is an important sink of ozone and is highly related to concentration of surface ozone and dry deposition velocity) also should be considered. ~~and advection (ADV, which is caused by the transport effects of wind fields).~~ More ~~More~~ information on processes analysis of the WRF-Chem system is available in Zhang et al. (2014), Gao et al., (2016) and the supplementary material., ~~and user guide of the WRF-Chem model.~~

Figure 5 illustrates the mean surface ozone concentrations and processes analysis results of the four cities during 07:00–18:00 (the results of each city are presented in Fig. ~~S3~~ S4 in the supplementary material). As shown in Fig. 5a, surface ozone began to be reduced by the impact of aerosols starting at 08:00 AM. From then, ozone reduction accumulated until the afternoon, with a maximum value of 11.7 ppb at 14:00. Similar to the processes analysis results of other studies (Kaser et al., 2017; Tang et al., 2017, Xing et al., 2017; Xu et al., 2018), the variation in surface ozone was mainly controlled by VMIX, DRY, and CHEM during the daytime (Fig. 5b and 5c). The contribution~~s~~ of CHEM at the surface ~~were~~ was generally below zero, which showed that the chemical consumption of ozone was equal to or stronger than the chemical production of ozone at the surface level. As an important removal of surface ozone, the contribution of DRY was always negative during daytime. ~~However~~On the contrary, the contribution of VMIX was positive~~,~~ which was the key factor leading to the increase in surface ozone during the daytime.

The reduction in surface ozone induced by aerosols can be decomposed into changes in process contributions (Exp2-Exp1), which are shown in Fig. 5d. The contributions of CHEM decreased significantly during the daytime, which was mainly due to the reduction in ozone chemical production caused by weakened ozone photochemistry. Distinct from the change in CHEM, the changes in DRY and VMIX were increased during daytime. ~~contribution of VMIX to surface ozone was enhanced during the same period.~~ From 8:00 to 14:00, the reduction in CHEM was more significant than the ~~enhancement~~ increases in VMIX and DRY, which made surface ozone continue decreasing during this period. After 14:00, the ~~enhancement~~ increases in VMIX and DRY almost counteracted the reduction in CHEM~~, which showed that ozone stopped decreasing~~. Quantitative results (Table 3) showed the ozone reduction and the accumulated changes in each process contribution at 14:00. The reduction in CHEM (-44.3 ppb) was much larger than the reduction in surface ozone (-11.7 ppb). Changes in VMIX (12.0 ppb), DRY (19.6 ppb), and ADV (0.9 ppb) were ~~enhanced~~ positive during this period. The ~~enhancement of~~ increase in ADV was relatively small, whereas the ~~enhancement~~ increases in ~~of~~ VMIX and DRY ~~was~~ were much ~~stronger~~larger, which partly offset the reduction in CHEM. Finally, because of considering all of these processes, the sum of these changes ($\sum_{i=8:00}^{14:00} NET\_DIF_i = -11.8$ ppb) almost ~~Considering the changes in all of the processes, the change in NET contribution finally~~ equaled to the reduction in ozone and ~~.~~the difference between $\Delta O_3^{at\ 14:00}$ and $\sum_{i=8:00}^{14:00} NET\_DIF_i$ was probably caused by numerical error. In addition, ~~Table~~ table 3 also clearly illustrates that the offset effect of VMIX and

DRY led to the inequality between the reduction in CHEM and reduction in surface ozone reported in the study of Li et al (2011b).

Because the contribution of DRY is usually negative to surface ozone, the increase of the change in DRY suggested that strength of dry deposition was weakened during daytime. Contribution from dry deposition is highly related to surface ozone concentration and dry deposition velocity. In Exp1 and Exp2, factors on dry deposition velocity such as land use and vegetation were not changed which indicated that dry deposition velocity didn't change (Wesely, 1989). However, the concentration of surface ozone decreased due to the impact of aerosols which finally leading to the weakened of dry deposition of ozone. By contrast, the increase of change in VMIX suggested the enhancement of vertical mixing process. Since vertical mixing occurring in the entire PBL, the change in VMIX can impact not only on surface ozone but also on the ozone aloft, which suggested that the change in ozone may also occur in the entire PBL.

3.3.2 Changes in ozone in the PBL induced by the decrease of photolysis rate

The averaged vertical changes of processes contributions of the four representative cities are presented in Fig. 6 (the results of each individual city are quite similar and are presented in Figs. ~~S4~~S5-~~S7~~ S8 in supplementary material). CHEM showed positive contributions aloft in both Exp1 and Exp2 (Fig. 6a and 6e, respectively), which resulted from strong ozone photochemical production. At the surface, it showed negative or weak positive contributions which was attributed to the much stronger chemical loss at the surface caused by ozone consuming species (i.e., NO). Figure 6i shows that the reduction in CHEM induced by aerosols occurred not only at the surface but also within the lowest 500 m during the daytime. VMIX (Fig. 6b and 6f) showed a negative contribution in the upper layer and a positive contribution in the lower layer, which indicated a high concentration of ozone aloft being entrained downward to the surface by turbulence during the daytime (Zhang and Rao, 1999; Gao et al., 2018a). The impact of aerosols enhanced the contributions of VMIX; thus, the change in VMIX showed a positive value within the lowest 300 m and negative values in the upper layer in the PBL. ADV (Fig. 6c and 6g) showed small contributions, and there was no significant change in ADV caused by the impact of aerosols. NET_DIF reflects the sum of the changes in all of the processes contributions and its distributions showed that, by affecting photolysis rate, the impact of aerosols led to the reduction in ozone occurring not only at the surface but also in the whole PBL (Fig. 6l). In the lower layer of the PBL, the reduction in CHEM was primarily responsible for the reduction in ozone, while the increase in VMIX partly counteracted the reduction in ozone. In the upper layer of the PBL, the decrease in VMIX played an important role in decreasing ozone aloft.

The contribution of VMIX is closely related to ozone vertical gradients and turbulence exchange coefficients. Studying the changes in the two factors is helpful to investigate the enhancement of VMIX induced by aerosols. As shown in Fig. 7a and 7b, via influencing the photolysis rate, the impact of aerosols didn't cause obvious changes in the exchange coefficients since the exchange coefficient profiles were almost the same as those from Exp1 and Exp2. However, the ozone gradient from Exp2 was larger than that from Exp1, which suggested that the enhancement of VMIX induced by aerosols was mainly associated with the increase in the ozone gradient. Because of the impact of aerosols, the chemical reduction in ozone was

more significant in the lower layer than in upper layer in the PBL (Fig. 6i), which led to smaller concentrations of ozone in the lower layer and consequently formed a larger vertical gradient (Fig. 7c). Therefore, high concentrations of ozone aloft would be entrained from the top of the PBL to the surface, which leaded to the enhancement in VMIX. In addition, similar features also occurred in each representative city which can be seen in Fig. ~~S8~~ S9 in the supplementary material.

3.4 The changes in ozone source contributions induced by aerosols via influencing the photolysis rate

Figure 8 illustrates the average ozone contributions from geographic source regions to surface ozone in the four cities from Exp1 and Exp2, and the changes in each ozone contribution induced by aerosols are also presented. For the representative cities, surface ozone was mainly contributed by local contribution and the contributions from adjacent source regions (left and middle columns in Fig. 8). For example, surface ozone over BJ and TJ was mainly contributed by ozone from themselves and Hebei Province. For SJZ and ZZ, ozone from their respective provinces (HB and HN) contributed more significantly than ozone from other regions did. In addition, $O_{3\text{-Inflow}}$, which can be approximately treated as background ozone (Gao et al., 2017), also showed an obvious contribution to surface ozone over each city.

With the impacts of aerosols, ozone from local and adjacent source region decreased more significantly than ozone from further source region did (right column in Fig. 8). For each city, the first four source regions that ozone contribution changed the most to the mean ozone concentration from 13:00 to 16:00 are listed in Table 4. For BJ and TJ, which are defined as independent source regions, ozone from local region decreased by -3.8 ppb and -3.8 ppb to BJ and TJ, respectively, which accounted for the greatest proportion. In addition, HB is adjacent to BJ and TJ, and ozone from HB decreased by 3.1 ppb and 3.0 ppb to ozone in BJ and TJ, respectively, which was more than ozone from long distance source regions did. SJZ and ZZ are the provincial capitals of HB and HN, ozone from HB and HN decreased by 4.6 ppb and 5.8 ppb to SJZ and ZZ, respectively. The reduction in ozone at the surface was mainly caused by the reduction in chemical production. For the ozone source apportionment method in this study, ozone chemical production can be traced to the source based on the ratio of ozone precursors from each source region. Due to the short lifetime of ozone precursors (i.e., NO_x), there will be more ozone precursors from local and adjacent source regions than which from further source regions. Thus, surface ozone from local and adjacent source regions decreased more with the impact of aerosols. At present, surface ozone has increased annually since the reduction in aerosols. Our ozone source apportionment results suggest that controlling ozone precursors from local and adjacent regions will be a more effective way to suppress the increase in surface ozone over CEC.

4 Conclusions

Currently, in China, the concentrations of surface ozone increase annually, which is considered closely related to the decrease in $PM_{2.5}$. Previous studies have summarized that, by decreasing the photolysis rate at the surface, the light extinction of aerosols could weaken ozone photochemistry and then directly reduce surface ozone. However, quantitative studies showed that the reduction in ozone net chemical production was much greater than the reduction in surface ozone,

which suggested that some other physical processes related to the variation in surface ozone were not discussed in previous studies.

To more clearly understand the impact of aerosols on ozone via affecting the photolysis rate, the WRF-Chem model was applied to simulate air pollutants over CEC in October 2018. Comprehensive model validations demonstrated the model performance in simulating air quality over CEC during this period. By comparing the results between the control and sensitive simulation, the mechanism of the impacts of aerosols on ozone was quantitatively studied. With the application of the ozone source apportionment method that we coupled into the WRF-Chem model, the impact of aerosol on the source-receptor relationship of ozone was also discussed.

Our results showed that, because of the light extinction of aerosols, the attenuation of incident solar irradiance caused the decrease in the photolysis rate below the PBL and then weakened ozone photochemistry. In this case, the net chemical production of ozone was significantly decreased within the lowest several hundred meters in the PBL. The decrease in surface ozone leading to the weakened of dry deposition of ozone which slowing down the decrease in surface ozone to a certain extent. More importantly, ~~The~~ the significant reduction in the net chemical production formed a larger ozone vertical gradient. And more air mass aloft with high concentration of ozone was entrained downward from the top of the PBL to the surface, which also partly counteracted the reduction in ozone net chemical production. Changes in the ~~two~~ three processes together led to the reduction in surface ozone. In addition, ozone in the upper layer of the PBL was also reduced, which was also induced by much ozone aloft being entrained downward. Therefore, by affecting the photolysis rate, the impact of aerosols can reduce ozone not only at the surface but also in the entire PBL during the daytime over CEC in this study.

The ozone source apportionment results showed that, for the four representative cities in CEC (BJ, TJ, SJZ, and ZZ), ozone from local and adjacent regions decreased by 6.9 ppb, 6.8 ppb, 4.6 ppb, and 5.8 ppb, respectively, which accounted for 41.4%–66.3% of the reduction in surface ozone in these cities. This suggested that the impact of aerosols on ozone from local and adjacent regions is more significant than that from long-distance regions. In recent years, with the implementation of the toughest-ever clean air policy in China, aerosols have decreased, whereas ozone increases year by year. Our results suggest that while controlling the concentrations of aerosols, controlling ozone precursors from local and adjacent regions is an effective way to suppress the increase in surface ozone.

Acknowledgements. This work was mainly supported by grants from the National Key Research and Development Program of China (2016YFA0602003), National Natural Science Foundation of China (41905114, 41961160728, 41575106), Science and Technology Planning Project of Guangdong Province of China (Grant 2017A050506003), Shenzhen Peacock Teams Plan (KQTD20180411143441009). Part of this work was supported by China Postdoctoral Science Foundation (2019M662169, 2019M662199). We also want to thank for the support from SUSTC Presidential Postdoctoral Fellowship. The simulated results in this study were calculated using computational resources provided by the Southern University of

Science and Technology. All the observations and model outputs mentioned in this study are available by contacting Ying Li via liy66@sustech.edu.cn.

References

Anger, A., Dessens, O., Xi, F. M., Barker, T., and Wu, R.: China's air pollution reduction efforts may result in an increase in surface ozone levels in highly polluted areas, Ambio, 45, 254-265, https://doi.org/10.1007/s13280-015-0700-6, 2016.

Bian, H., Han, S. Q., Tie, X. X., Sun, M. L., and Liu, A. X.: Evidence of impact of aerosols on surface ozone concentration in Tianjin, China, Atmos. Environ., 41, 4672-4681, https://doi.org/10.1016/j.atmosenv.2007.03.041, 2007.

Bohn, B., Kraus, A., Muller, M., and Hofzumahaus, A.: Measurement of atmospheric $O_3 \rightarrow O(^1D)$ photolysis frequencies using filterradiometry, J. Geophys. Res.-Atmos., 109, D10S90, https://doi.org/10.1029/2003JD004319, 2004.

Cai, Y. F., Wang, T. J., and Xie, M.: Impacts of atmospheric particles on surface ozone in Nanjing (In Chinese), Climatic Environment Research, 18, 251-260, 2013.

Castro, T., Madronich, S., Rivale, S., Muhlia, A., and Mar, B.: The influence of aerosols on photochemical smog in Mexico City, Atmos. Environ., 35, 1765-1772, https://doi.org/10.1016/S1352-2310(00)00449-0, 2001.

Chen, F., and Dudhia, J.: Coupling an advanced land surface-hydrology model with the Penn State-NCAR MM5 modeling system. Part I: Model implementation and sensitivity, Mon. Weather Rev., 129, 569-585, 2001.

Crutzen, P.: A discussion of the chemistry of some minor constituents in the stratosphere and troposphere, Pure and ~~Applied~~ Appl. ~~Geophysics~~Geophys., 106, 1385-1399, https://doi.org/10.1007/bf00881092, 1973.

Deng, X. J., Zhou, X. J., Tie, X. X., Wu, D., Li, F., Tan, H. B., and Deng, T.: Attenuation of ultraviolet radiation reaching the surface due to atmospheric aerosols in Guangzhou, Chinese Sci. Bull., 57, 2759-2766, https://doi.org/10.1007/s11434-012-5172-5, 2012.

Dickerson, R. R., Kondragunta, S., Stenchikov, G., Civerolo, K. L., Doddridge, B. G., and Holben, B. N.: The impact of aerosols on solar ultraviolet radiation and photochemical smog, Science, 278, 827-830, https://doi.org/10.1126/science.278.5339.827, 1997.

Ding, A. J., Huang, X., Nie, W., Sun, J. N., Kerminen, V. M., Petaja, T., Su, H., Cheng, Y. F., Yang, X. Q., Wang, M. H., Chi, X. G., Wang, J. P., Virkkula, A., Guo, W. D., Yuan, J., Wang, S. Y., Zhang, R. J., Wu, Y. F., Song, Y., Zhu, T., Zilitinkevich, S., Kulmala, M., and Fu, C. B.: Enhanced haze pollution by black carbon in megacities in China, Geophys. Res. Lett., 43, 2873-2879, https://doi.org/10.1002/2016GL067745, 2016.

Emery, C., Tai, E., and Yarwood, G.: Enhanced meteorological modeling and performance evaluation for two Texas ozone episodes, in: Prepared for the Texas Natural Resource Conservation Commission, ENVIRON International Corporation, Novato, CA, USA, 2001

ENVIRON, CAMx 5.4 Manual, http://www.camx.com/, 2011.

EPA, U.S.: Guidance on the Use of Models and Other Analyses in Attainment Demonstrations for the 8-hour Ozone NAAQS, EPA-454/R-05-002, 2005.

EPA, U.S.: Guidance on the Use of Models and Other Analyses for Demonstrating Attainment of Air Quality Goals for Ozone, $PM_{2.5}$, and Regional Haze, EPA-454/B-07-002, 2007.

Gao, J. H., Zhu, B., Xiao, H., Kang, H. Q., Hou, X. W., Yin, Y., Zhang, L., and Miao, Q.: Diurnal variations and source apportionment of ozone at the summit of Mount Huang, a rural site in Eastern China, Environ. Pollut., 222, 513-522, https://doi.org/10.1016/j.envpol.2016.11.031, 2017.

Gao, J. H., ~~Bin~~Zhu, ~~Z~~B., Xiao, H., Kang, H. Q., Hou, X. W., and Shao, P.: A case study of surface ozone source apportionment during a high concentration episode, under frequent shifting wind conditions over the Yangtze River Delta, China, Sci. Total Environ., 544, 853-863, https://doi.org/10.1016/j.scitotenv.2015.12.039, 2016.

Gao, J. H., Zhu, B., Xiao, H., Kang, H. Q., Pan, C., Wang, D. D., and Wang, H. L.: Effects of black carbon and boundary layer interaction on surface ozone in Nanjing, China, Atmos. Chem. Phys., 18, 7081-7094, https://doi.org/10.5194/acp-18-7081-2018, 2018a.

Gao, M., Han, Z. W., Liu, Z. R., Li, M., Xin, J. Y., Tao, Z. N., Li, J. W., Kang, J. E., Huang, K., Dong, X. Y., Zhuang, B. L., Li, S., Ge, B. Z., Wu, Q. Z., Cheng, Y. F., Wang, Y. S., Lee, H. J., Kim, C. H., Fu, J. S. S., Wang, T. J., Chin, M. A., Woo, J. H., Zhang, Q., Wang, Z. F., and Carmichael, G. R.: Air quality and climate change, Topic 3 of the Model Inter-Comparison Study for Asia Phase III (MICS-Asia III) - Part 1: Overview and model evaluation, Atmos. Chem. Phys., 18, 4859-4884, https://doi.org/10.5194/acp-18-4859-2018, 2018b.

Gery, M. W., Whitten, G. Z., Killus, J. P., and Dodge, M. C.: A p~~P~~hotochemical ~~Kinetics~~ kinetics ~~Mechanism~~ mechanism for ~~Urban~~ urban ~~And~~ and ~~Regional~~ regional ~~Scale~~ scale ~~Computer~~ computer ~~Modeling~~modeling, J. Geophys. Res.-Atmos., 94, 12925-12956, https://doi.org/~~Doi~~ 10.1029/Jd094id10p12925, 1989.

Gleckler, P. J., Taylor, K. E., and Doutriaux, C.: Performance metrics for climate models, J. Geophys. Res.-Atmos., 113, D06104, https://doi.org/10.1029/2007jd008972, 2008.

Grell, G. A., Peckham, S. E., Schmitz, R., McKeen, S. A., Frost, G., Skamarock, W. C., and Eder, B.: Fully coupled "online" chemistry within the WRF model, Atmos. Environ., 39, 6957-6975, https://doi.org/10.1016/j.atmosenv.2005.04.027, 2005.

Guenther, A., Karl, T., Harley, P., Wiedinmyer, C., Palmer, P. I., and Geron, C.: Estimates of global terrestrial isoprene emissions using MEGAN (Model of Emissions of Gases and Aerosols from Nature), Atmos. Chem. Phys., 6, 3181-3210, 10.5194/acp-6-3181-2006, 2006.

Haagen-Smit, A. J., and Fox, M. M.: Photochemical ozone formation with hydrocarbons and automobile exhaust, Air Repair, 4, 105-136, https://doi.org/10.1080/00966665.1954.10467649, 1954.

Hansen, J., Sato, M., and Ruedy, R.: Radiative forcing and climate response, J. Geophys. Res.-Atmos., 102, 6831-6864, https://doi.org/10.1029/96jd03436, 1997.

Hofzumahaus, A., Kraus, A., and Muller, M.: Solar actinic flux spectroradiometry: a technique for measuring photolysis frequencies in the atmosphere, Appl. Optics., 38, 4443-4460, https://doi.org/10.1364/Ao.38.004443, 1999.

Hong, S. Y., Noh, Y., and Dudhia, J.: A new vertical diffusion package with an explicit treatment of entrainment processes, Mon. Weather Rev., 134, 2318-2341, https://doi.org/10.1175/Mwr3199.1, 2006.

Hu, J. L., Chen, J. J., Ying, Q., and Zhang, H. L.: One-year simulation of ozone and particulate matter in China using WRF/CMAQ modeling system, Atmos. Chem. Phys., 16, 10333-10350, https://doi.org/10.5194/acp-16-10333-2016, 2016.

Hu, X. M., Xue, M., Kong, F. Y., and Zhang, H. L.: Meteorological ~~Conditions~~ conditions ~~During~~ during an ~~Ozone~~ ozone ~~Episode~~ episode in Dallas-Fort Worth, Texas, and ~~Impact~~ impact of ~~Their~~ their ~~Modeling~~ modeling ~~Uncertainties~~ uncertainties on ~~Air~~ air ~~Quality~~ quality ~~Prediction~~prediction, J. Geophys. Res.-Atmos., 124, 1941-1961, https://doi.org/10.1029/2018JD029791, 2019.

Iacono, M. J., Delamere, J. S., Mlawer, E. J., Shephard, M. W., Clough, S. A., and Collins, W. D.: Radiative forcing by long-lived greenhouse gases: Calculations with the AER radiative transfer models, J. Geophys. Res.-Atmos., 113, D13, https://doi.org/10.1029/2008jd009944, 2008.

Jacobson, M. Z.: Studying the effects of aerosols on vertical photolysis rate coefficient and temperature profiles over an urban airshed, J. Geophys. Res.-Atmos., 103, 10593-10604, https://doi.org/10.1029/98jd00287, 1998.

Kang, H. Q., Zhu, B., Gao, J. H., He, Y., Wang, H. L., Su, J. F., Pan, C., Zhu, T., and Yu, B.: Potential impacts of cold frontal passage on air quality over the Yangtze River Delta, China, Atmos. Chem. Phys., 19, 3673-3685, https://doi.org/10.5194/acp-19-3673-2019, 2019.

Kaser, L., Patton, E. G., Pfister, G. G., Weinheimer, A. J., Montzka, D. D., Flocke, F., Thompson, A. M., Stauffer, R. M., and Halliday, H. S.: The effect of entrainment through atmospheric boundary layer growth on observed and modeled surface ozone in the Colorado Front Range, J. Geophys. Res.-Atmos., 122, 6075-6093, https://doi.org/10.1002/2016JD026245, 2017.

Kwok, R. H. F., Fung, J. C. H., Lau, A. K. H., and Fu, J. S.: Numerical study on seasonal variations of gaseous pollutants and particulate matters in Hong Kong and Pearl River Delta Region, J. Geophys. Res.-Atmos., 115, D16308, https://doi.org/10.1029/2009jd012809, 2010.

Lamarque, J. F., Emmons, L. K., Hess, P. G., Kinnison, D. E., Tilmes, S., Vitt, F., Heald, C. L., Holland, E. A., Lauritzen, P. H., Neu, J., Orlando, J. J., Rasch, P. J., and Tyndall, G. K.: CAM-chem: description and evaluation of interactive atmospheric chemistry in the Community Earth System Model, Geosci. Model. Dev., 5, 369-411, https://doi.org/10.5194/gmd-5-369-2012, 2012.

Li, G., Bei, N., Tie, X. X., and Molina, L. T.: Aerosol effects on the photochemistry in Mexico City during MCMA-2006/MILAGRO campaign, Atmos. Chem. Phys., 11, 5169-5182, https://doi.org/10.5194/acp-11-5169-2011, 2011a.

Li, G. H., Zhang, R. Y., Fan, J. W., and Tie, X. X.: Impacts of black carbon aerosol on photolysis and ozone, J. Geophys. Res.-Atmos., 110, D23206, https://doi.org/10.1029/2005jd005898, 2005.

Li, J., Wang, Z., Wang, X., Yamaji, K., Takigawa, M., Kanaya, Y., Pochanart, P., Liu, Y., Irie, H., Hu, B., Tanimoto, H., and Akimoto, H.: Impacts of aerosols on summertime tropospheric photolysis frequencies and photochemistry over Central Eastern China, Atmos. Environ., 45, 1817-1829, https://doi.org/10.1016/j.atmosenv.2011.01.016, 2011b.

Li, K., Jacob, D. J., Liao, H., Shen, L., Zhang, Q., and Bates, K. H.: Anthropogenic drivers of 2013-2017 trends in summer surface ozone in China, P. Natl. Acad. Sci. USA, 116, 422-427, https://doi.org/10.1073/pnas.1812168116, 2019a.

Li, K., Jacob, D. J., Liao, H., Zhu, J., Shah, V., Shen, L., Bates, K. H., Zhang, Q., and Zhai, S. X.: A two-pollutant strategy for improving ozone and particulate air quality in China, Nature Nat. GeoscienceGeosci., 12, 906-910, https://1-5, doi.org/10.1038/s41561-019-0464-x, 2019b.

Li, M., Zhang, Q., Kurokawa, J., Woo, J. H., He, K. B., Lu, Z. F., Ohara, T., Song, Y., Streets, D. G., Carmichael, G. R., Cheng, Y. F., Hong, C. P., Huo, H., Jiang, X. J., Kang, S. C., Liu, F., Su, H., and Zheng, B.: MIX: a mosaic Asian anthropogenic emission inventory under the international collaboration framework of the MICS-Asia and HTAP, Atmos. Chem. Phys., 17, 935-963, https://doi.org/10.5194/acp-17-935-2017, 2017a.

Li, Z. Q., Guo, J. P., Ding, A. J., Liao, H., Liu, J. J., Sun, Y. L., Wang, T. J., Xue, H. W., Zhang, H. S., and Zhu, B.: Aerosol and boundary-layer interactions and impact on air quality, Natl. Sci. Rev., 4, 810-833, https://doi.org/10.1093/nsr/nwx117, 2017b.

Lin, Y. L., Farley, R. D., and Orville, H. D.: Bulk parameterization of the snow field in a cloud model, J. Clim. Appl. Meteorol., 22, 1065-1092, https://doi.org/10.1175/1520-0450(1983)022<1065:BPOTSF>2.0.CO;2, 1983.

Monks, P. S., Archibald, A. T., Colette, A., Cooper, O., Coyle, M., Derwent, R., Fowler, D., Granier, C., Law, K. S., Mills, G. E., Stevenson, D. S., Tarasova, O., Thouret, V., von Schneidemesser, E., Sommariva, R., Wild, O., and Williams, M. L.: Tropospheric ozone and its precursors from the urban to the global scale from air quality to short-lived climate forcer, Atmos. Chem. Phys., 15, 8889-8973, https://doi.org/10.5194/acp-15-8889-2015, 2015.

Shao, M., Tang, X. Y., Zhang, Y. H., and Li, W. J.: City clusters in China: air and surface water pollution, Front. Ecol. Environ., 4, 353-361, https://doi.org/10.1890/1540-9295(2006)004[0353:CCICAA]2.0.CO;2, 2006.

Skamarock, W., Klemp, J. B., Dudhia, J., Gill, D. O., Barker, D. M., Duda, M., Huang, X. Y., Wang, W., and Powers, J. G.: A description of the advanced research WRF version 3, NCAR technical note NCAR/TN/u2013475, 2008.

Tang, G. Q., Zhu, X. W., Xin, J. Y., Hu, B., Song, T., Sun, Y., Zhang, J. Q., Wang, L. L., Cheng, M. T., Chao, N., Kong, L. B., Li, X., and Wang, Y. S.: Modelling study of boundary-layer ozone over northern China - Part I: Ozone budget in summer, Atmos. Res., 187, 128-137, https://doi.org/10.1016/j.atmosres.2016.10.017, 2017.

Taylor, K. E.: Summarizing multiple aspects of model performance in a single diagram, J. Geophys. Res.-Atmos., 106, 7183-7192, https://doi.org/10.1029/2000jd900719, 2001.

Tie, X. X., Geng, F., Guenther, A., Cao, J., Greenberg, J., Zhang, R., Apel, E., Li, G., Weinheimer, A., Chen, J., and Cai, C.: Megacity impacts on regional ozone formation: observations and WRF-Chem modeling for the MIRAGE-Shanghai field campaign, Atmos. Chem. Phys., 13, 5655-5669, https://doi.org/10.5194/acp-13-5655-2013, 2013.

Wang, J., Allen, D. J., Pickering, K. E., Li, Z. Q., and He, H.: Impact of aerosol direct effect on East Asian air quality during the EAST-AIRE campaign, J. Geophys. Res.-Atmos., 121, 6534-6554, https://doi.org/10.1002/2016JD025108, 2016.

Wang, J. D., Zhao, B., Wang, S. X., Yang, F. M., Xing, J., Morawska, L., Ding, A. J., Kulmala, M., Kerminen, V. M., Kujansuu, J., Wang, Z. F., Ding, D. A., Zhang, X. Y., Wang, H. B., Tian, M., Petaja, T., Jiang, J. K., and Hao, J. M.: Particulate matter pollution over China and the effects of control policies, Sci. Total Environ., 584, 426-447, https://doi.org/10.1016/j.scitotenv.2017.01.027, 2017.

Wang, L. T., Wei, Z., Yang, J., Zhang, Y., Zhang, F. F., Su, J., Meng, C. C., and Zhang, Q.: The 2013 severe haze over southern Hebei, China: model evaluation, source apportionment, and policy implications, Atmos. Chem. Phys., 14, 3151-3173, https://doi.org/10.5194/acp-14-3151-2014, 2014a.

Wang, W. J., Li, X., Shao, M., Hu, M., Zeng, L. M., Wu, Y. S., and Tan, T. Y.: The impact of aerosols on photolysis frequencies and ozone production in Beijing during the 4-year period 2012-2015, Atmos. Chem. Phys., 19, 9413-9429, https://doi.org/10.5194/acp-19-9413-2019, 2019.

Wang, Y. G., Ying, Q., Hu, J. L., and Zhang, H. L.: Spatial and temporal variations of six criteria air pollutants in 31 provincial capital cities in China during 2013-2014, Environ. Int., 73, 413-422, https://doi.org/10.1016/j.envint.2014.08.016, 2014b.

Wang, Z. F., Li, J., Wang, Z., Yang, W. Y., Tang, X., Ge, B. Z., Yan, P. Z., Zhu, L. L., Chen, X. S., Chen, H. S., Wand, W., Li, J. J., Liu, B., Wang, X. Y., Wand, W., Zhao, Y. L., Lu, N., and Su, D. B.: Modeling study of regional severe hazes over mid-eastern China in January 2013 and its implications on pollution prevention and control, Sci. China Earth Sci., 57, 3-13, https://doi.org/10.1007/s11430-013-4793-0, 2014c.

Wesely, M. L.: Parameterization of surface resistances to gaseous dry deposition in regional-scale numerical-models, Atmos. Environ., 23, 1293-1304, https://doi.org/10.1016/0004-6981(89)90153-4, 1989.

Wild, O., Zhu, X., and Prather, M. J.: Fast-jJ: Accurate simulation of in- and below-cloud photolysis in tropospheric chemical models, J. Atmos. Chem., 37, 245-282, https://doi.org/10.1023/A:1006415919030, 2000.

Xing, J., Wang, J. D., Mathur, R., Wang, S. X., Sarwar, G., Pleim, J., Hogrefe, C., Zhang, Y. Q., Jiang, J. K., Wong, D. C., and Hao, J. M.: Impacts of aerosol direct effects on tropospheric ozone through changes in atmospheric dynamics and photolysis rates, Atmos. Chem. Phys., 17, 9869-9883, https://doi.org/10.5194/acp-17-9869-2017, 2017.

Xu, Z. N., Huang, X., Nie, W., Shen, Y. C., Zheng, L. F., Xie, Y. N., Wang, T. Y., Ding, K., Liu, L. X., Zhou, D. R., Qi, X. M., and Ding, A. J.: Impact of Biomass Burning and Vertical Mixing of Residual-Layer Aged Plumes on Ozone in the Yangtze River Delta, China: A Tethered-Balloon Measurement and Modeling Study of a Multiday Ozone Episode, J. Geophys. Res.-Atmos., 123, 11786-11803, https://doi.org/10.1029/2018JD028994, 2018.

Yarwood, G., Morris, R. E., Yocke, M. A., Hogo, H., and Chico, T.: Development of a methodology for source apportionment of ozone concentrations estimates from a photochemical grid model, Air and Waste management association, Pittsburgh USA, 15222, 2006.

Zaveri, R. A., and Peters, L. K.: A new lumped structure photochemical mechanism for large - scale applications, J. ~~ournal of Geophysical~~ Geophys. ~~Research~~ Res. : ~~-Atmospheres~~ Atmos., 104, 30387-30415, https://doi.org/10.1029/1999JD900876, 1999.

Zaveri, R. A., Easter, R. C., Fast, J. D., and Peters, L. K.: Model for simulating aerosol interactions and chemistry (MOSAIC), J. Geophys. Res.-Atmos., 113, D13204, https://doi.org/10.1029/2007jd008782, 2008.

Zhang, H., DeNero, S. P., Joe, D. K., Lee, H. H., Chen, S. H., Michalakes, J., and Kleeman, M. J.: Development of a source oriented version of the WRF/Chem model and its application to the California regional $PM_{10}/PM_{2.5}$ air quality study, Atmos. Chem. Phys., 14, 485-503, https://doi.org/10.5194/acp-14-485-2014, 2014.

Zhang, J., and Rao, S. T.: The role of vertical mixing in the temporal evolution of ground-level ozone concentrations, J. Appl. Meteorol., 38, 1674-1691, https://doi.org/10.1175/1520-0450(1999)038<1674:trovmi>2.0.CO;2, 1999.

Zhu, B., Kang, H. Q., Zhu, T., Su, J. F., Hou, X. W., and Gao, J. H.: Impact of Shanghai urban land surface forcing on downstream city ozone chemistry, J. Geophys. Res.-Atmos., 120, 4340-4351, https://doi.org/10.1002/2014JD022859, 2015.

530 **Table 1: Major configuration options of WRF-Chem used for this study.**

Item	Selection	Reference
Photolysis scheme	Fast-J photolysis	Wild et al., (2000)
Long wave scheme	RRTMG[a]	Iacono et al., (2008)
Short wave scheme	RRTMG[a]	Iacono et al., (2008)
Microphysics scheme	Lin scheme	Lin et al., (1983)
Land surface scheme	Noah land surface model	Chen and Dudhia (2001)
PBL scheme	Yonsei University (YSU) scheme	Hong et al., (2006)
Dry deposition scheme	Wesely scheme	Wesely (1989)

[a] RRTMG=Rapid Radiative Transfer Model for GCMs

Table 2: Mean model performance metrics for meteorological factors and air pollutants. The values that do not meet the benchmarks are denoted in bold.

Variables	IOA	MB	RMSE	MNB	MFB
T2 (°C)	0.93 (≥0.8)	**0.71** ([-0.5,0.5])	2.42	-0.01	-0.09
WS (m s^{-1})	0.78 (≥0.6)	-0.42 ([-0.5,0.5])	1.26 (≤2)	-0.03	-0.28
WD (°)	0.89	6.59 ([-10,10])	-0.42	1.64	0.02
O_3 (μg m^{-3})	0.84	-6.51	27.68	**0.16** ([-0.15,0.15])	-0.24
NO_2 (μg m^{-3})	0.73	-5.97	23.39	-0.13	-0.35
$PM_{2.5}$ (μg m^{-3})	0.74	8.11	28.75	0.34	0.08 ([-0.6,0.6])

Table 3: The reduction of surface ozone at 14:00 and the corresponding accumulated changes of processes contributions.

$\Delta O_3^{at\ 14:00}$	$\sum_{i=8:00}^{14:00} CHEM\_DIF_i$	$\sum_{i=8:00}^{14:00} VMIX\_DIF_i$	$\sum_{i=8:00}^{14:00} DRY\_DIF_i$	$\sum_{i=8:00}^{14:00} ADV\_DIF_i$	$\sum_{i=8:00}^{14:00} NET\_DIF_i$
-11.7 ppb	~~-44.2~~ -44.3 ppb	~~31.6~~12.0 ppb	19.6 ppb	0.9 ppb	-11.8 ~~-11.7~~ ppb

Table 4: The first four source regions that ozone contribution changes the most to the mean ozone concentration from 13:00 to 16:00 in each city. Local region and source region where the city located in are denoted as bold.

City	ΔOzone	ΔContribution			
		1st	2nd	3rd	4th
BJ	-10.4 ppb	**BJ** -3.8 ppb (36.5%)	HB -3.1 ppb (29.8%)	TJ -1.3 ppb (12.5%)	SD -0.5 ppb (4.8%)
TJ	-12.3 ppb	**TJ** -3.8 ppb (30.9%)	HB -3.0 ppb (24.4%)	SD -1.9 ppb (15.4%)	SIB -0.8 ppb (6.5%)
SJZ	-11.1 ppb	**HB** -4.6 ppb (41.4%)	HN -1.5 ppb (13.5%)	SIB -0.9 ppb (8.1%)	$O_{3\text{-inflow}}$ -0.8 ppb (7.2%)
ZZ	-9.8 ppb	**HN** -5.8 ppb (59.2%)	JS -0.9 ppb (9.2%)	SIB -0.6 ppb (6.1%)	SH -0.4 ppb (4.1%)

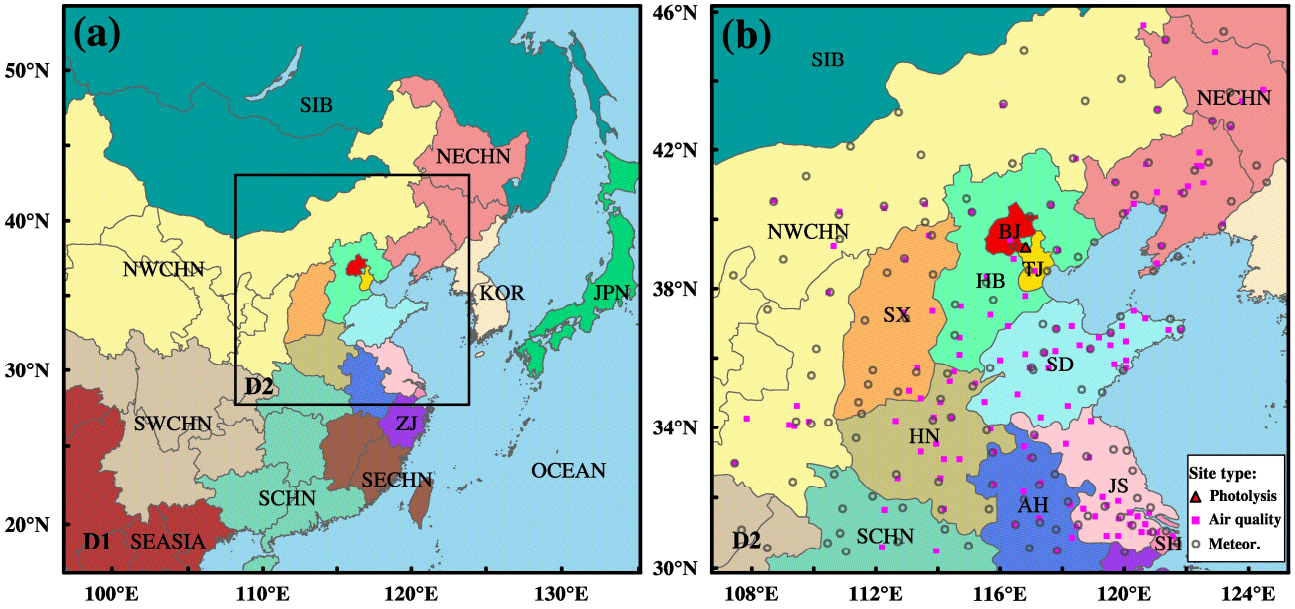

Figure 1: Model domain. Hundreds of observations are used for model validation, locations and types of the observation stations are shown in (b). The figure also shows the source regions denoted by different colors.

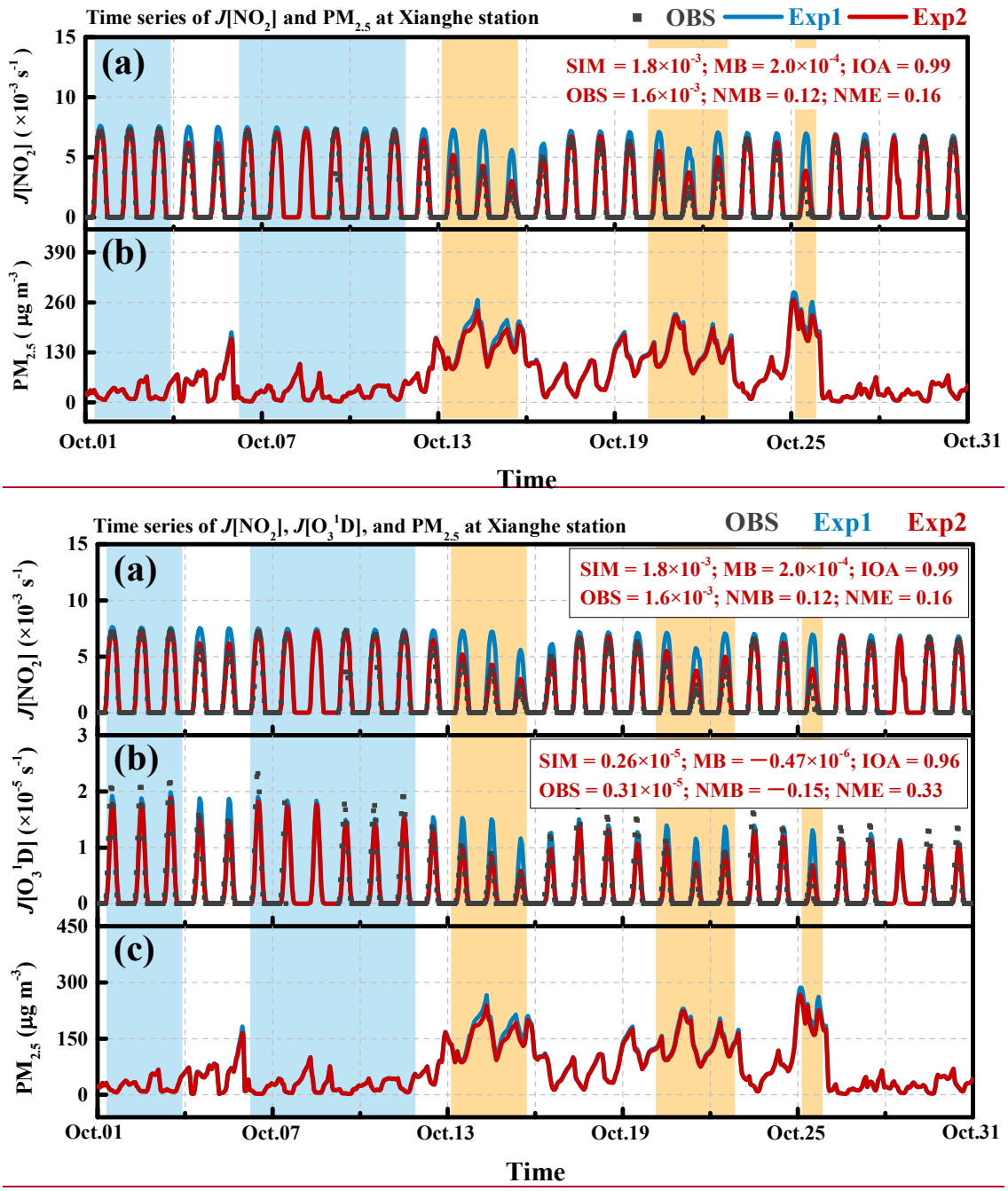

Figure 2: Time series of simulated $J[NO_2]$ (a), $J[O_3{}^1D]$ (b), and $PM_{2.5}$ (~~b~~c) at Xianghe station.

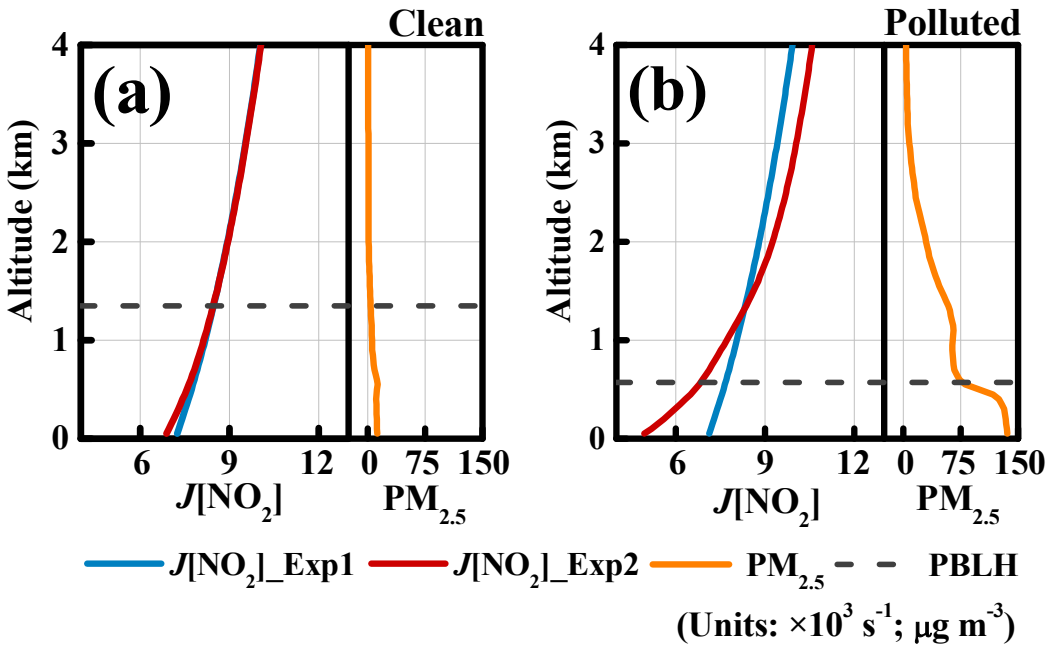

Figure 3: Mean profiles of $J[NO_2]$ (red and blue lines) and $PM_{2.5}$ (orange line) at 12:00 in clean days (a) and polluted days (b). Profiles of $J[NO_2]$ in Exp1 and Exp2 are denoted by red and blue, respectively. Mean PBL heights (PBLH; black dashed line) of the two kinds of days are also presented in (a) and (b), respectively.

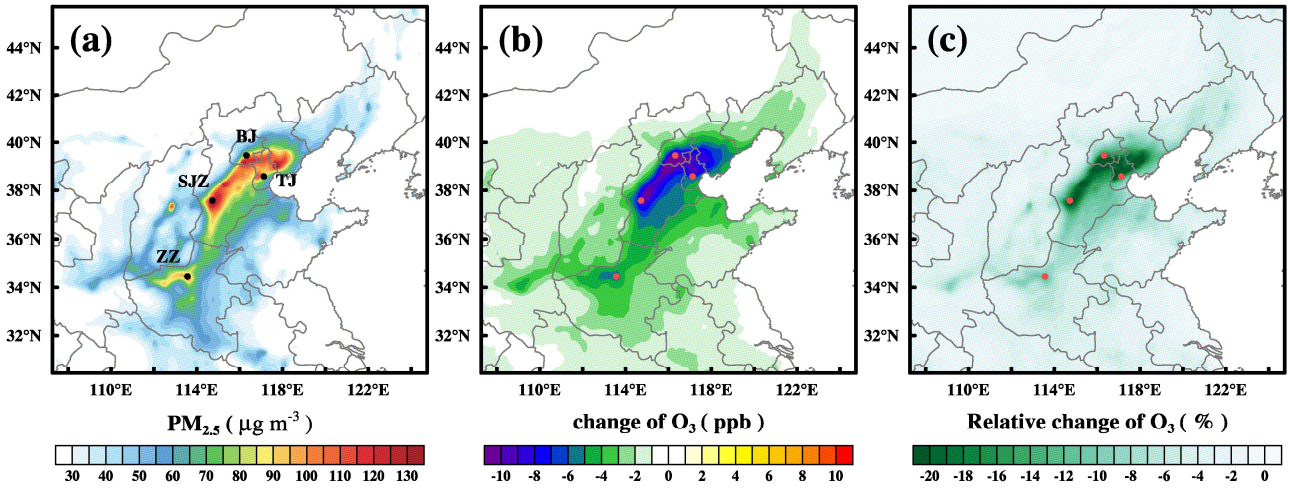

Figure 4: Mean distributions of $PM_{2.5}$ (a), change of O_3 (b) and relative change of O_3 (c) at surface over CEC during high $PM_{2.5}$ episodes. Dots denote the four typical cities in CEC, BJ=Beijing; TJ=Tianjin; SJZ=Shijiahuang; ZZ=Zhengzhou

560

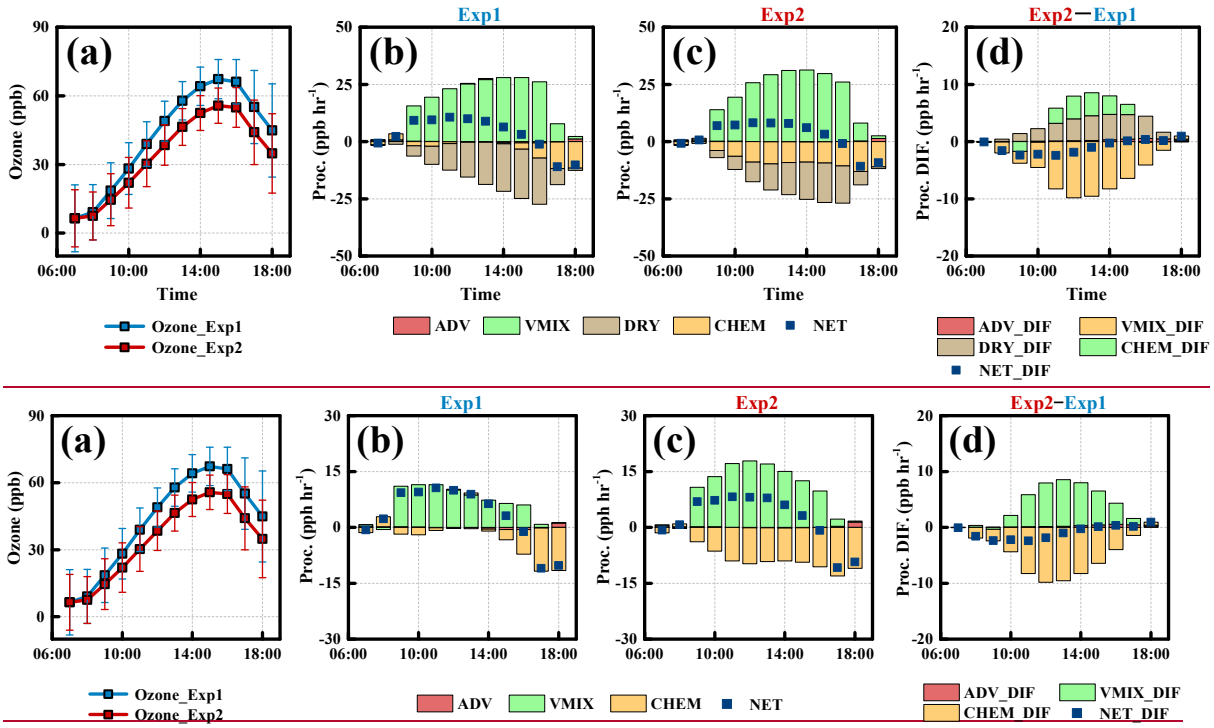

Figure 5: Averaged surface ozone concentrations and processes analysis results of the four cities at daytime. Mean ~~at surface~~ ozone concentrations from Exp1 and Exp2 are presented in (a); the corresponding ~~(a),~~ hourly processes contributions ~~and net contribution of ozone in~~from Exp1 ~~(b)~~ and Exp2 ~~(c)~~are presented in (b) and (c);~~,~~ the changes of each ~~of hourly~~ process~~es contributions and net contribution~~ induced by aerosol (Exp2-Exp1)– are presented in (d)~~at daytime~~. CHEM = chemistry, VMIX+DRY = vertical mixing and dry deposition, ADV = advection, NET = CHEM + VMIX + DRY + ADV. Changes of each process contribution and NET contribution are denoted by CHEM_DIF, VMIX+DRY_DIF, ADV_DIF and NET_DIF, respectively.

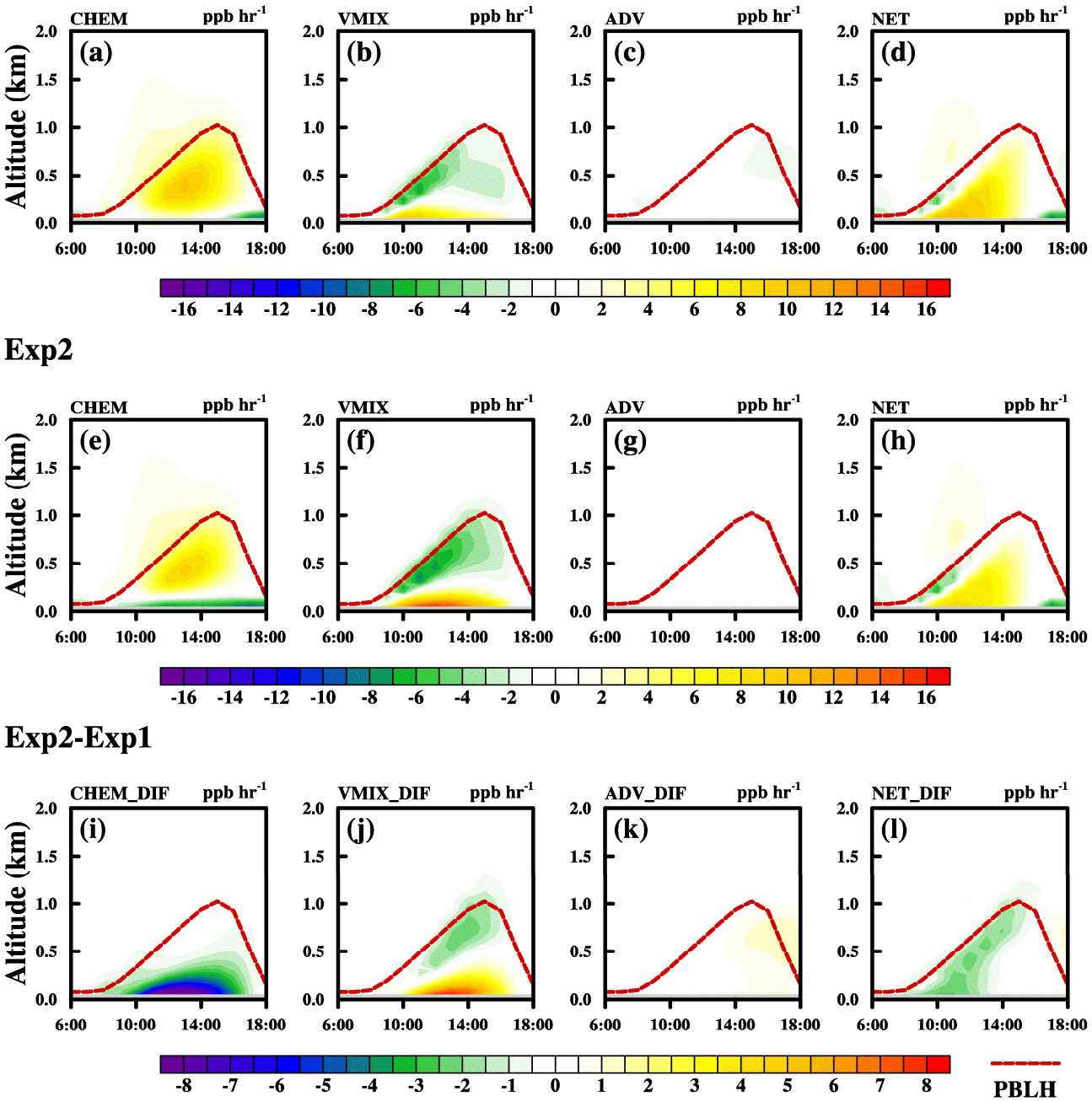

Figure 6: Averaged vertical distributions of processes contributions in function with time from 06:00 to 18:00 LT. Data is spatially sampled. All the grids within the administrative regions of the four cities are collected and averaged which can represent the situation of the four cities. (a)-(d) for processes contributions from ~~CAS~~Exp1; (e)-(h) for processes contributions from ~~CAS~~Exp2; (i)-(l) for the changes of each process contribution due to aerosols (Exp2-Exp1). Red dash lines denote PBLH.

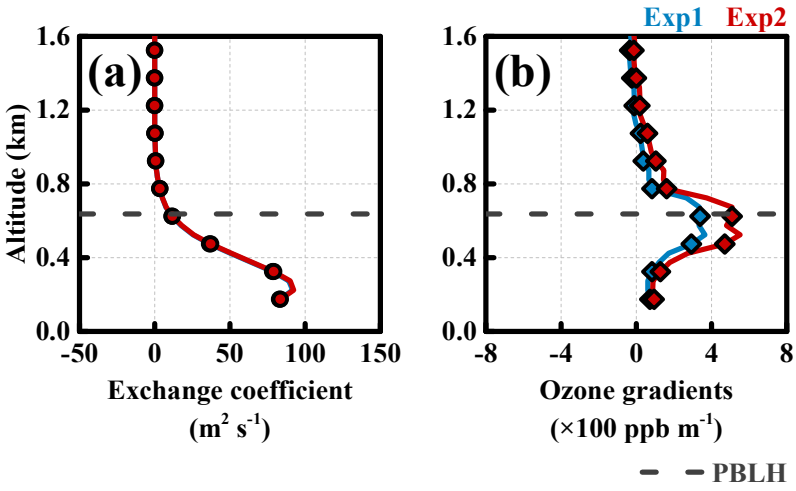

Figure 7: Averaged vertical profiles of ~~(a)~~ turbulence exchange coefficients (a) and ~~(b)~~ vertical gradients of ozone (b) of the four cities ~~from Exp1 and Exp2~~ at 12:00 AM. Dark gray dash line denotes PBLH at this time.

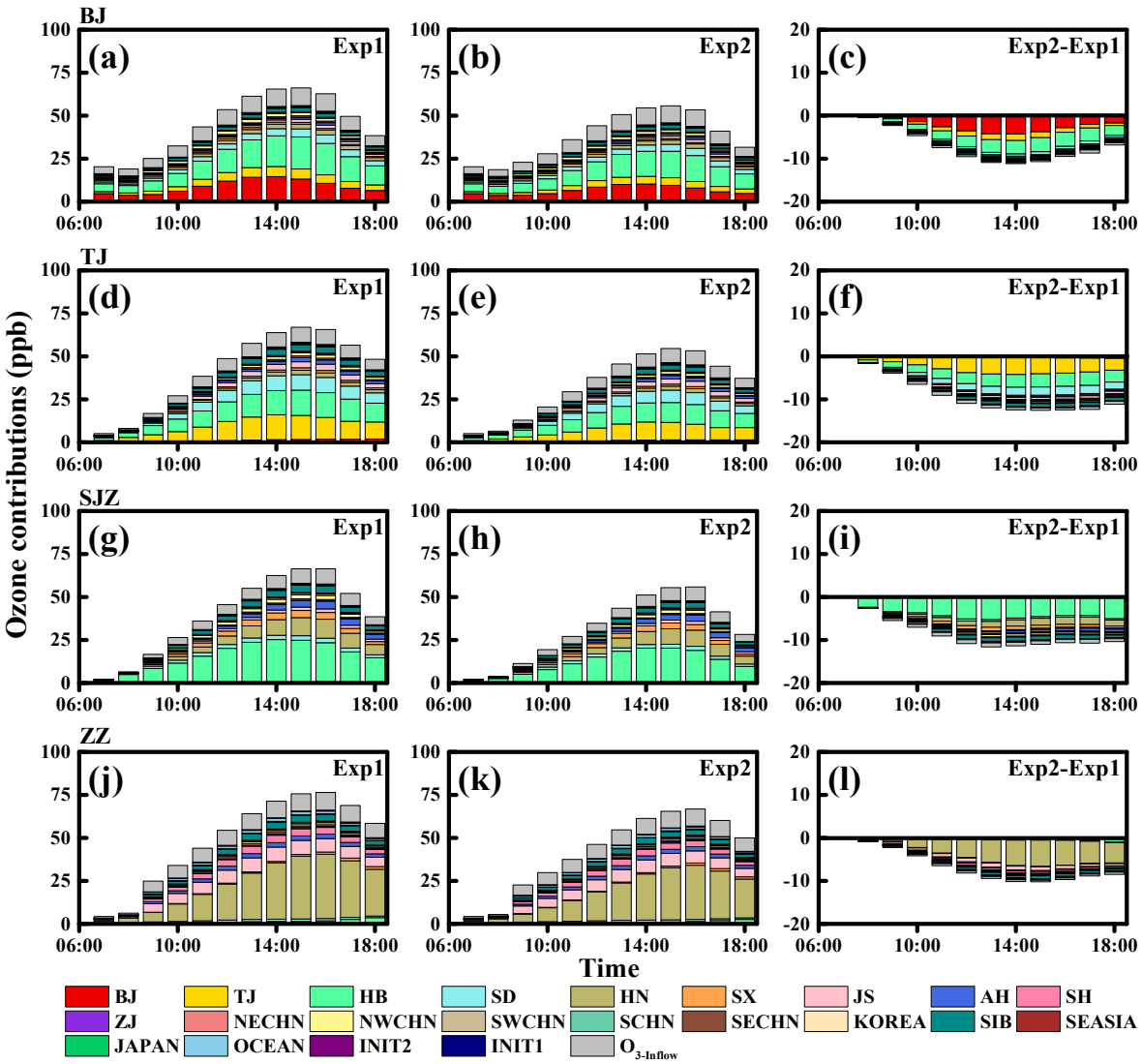

580

Figure 8: Averaged ozone contributions and changes induced by aerosols from geographical source regions to BJ (a)-(c), TJ (d)-(f), SJZ (g)-(i) and ZZ (j)-(l) from 07:00 to 18:00 LT.